Project Number: 640176

Project Acronym: BACI

Project title: Detecting changes in essential ecosystem and biodiversity properties- towards a Biosphere Atmosphere Change Index

Deliverable 7.2

Deliverable 7.2: Report on global demand and for land-based products, and inputs in the land system in decadal time series at the global level
Due date: Month 28 (two weeks extension granted)
Date: 10.08.2017
Authors: Maria Niedertscheider, Thomas Kastner, Christoph Plutzar, Karl-Heinz Erb
Institution: Institute of Social Ecology (UNI-KLU)

1. Introduction

The socio-economic dimension of Biosphere-Atmosphere changes

Land use provides the basis of human sustenance, but changes in land cover and land use are also pervasive drivers of global biosphere-atmosphere change (Millenium Ecosystem Assessment 2005; Foley et al. 2005). Today, land use affects more than three quarters of the earth's terrestrial ecosystems (Erb et al. 2007; Ellis et al. 2013; Luyssaert et al. 2014) and has led to annual release of carbon from biota and soils of 4.03 ± 2.93 GtCO2/year (billion tons of CO2 per year) globally over the last four centuries (Smith et al. 2014b).

Likewise, intensification of land use has widespread detrimental consequences such as eutrophication, air pollution, greenhouse gas emissions, topsoil loss, or biodiversity loss (Matson and Vitousek 2006; Foley et al. 2005; IAASTD 2009; Lindenmayer et al. 2012). These problems may be aggravated in the future due to anticipated increases in the demand for food, fibre, shelter, bioenergy, and freshwater, and the need to mitigate climate change, e.g. by limiting further conversions of forests to agriculture or the provision of bioenergy (Smith et al. 2014b). Because fertile land is increasingly scarce and the competition for it increases, decoupling production increases from the environmental impacts of land-based production related to land expansion is therefore a central sustainability challenge of the twenty-first century (Lambin and Meyfroidt 2011; Tilman et al. 2011; Garnett et al. 2013; Verburg et al. 2013).

However, many knowledge gaps relate to the impacts of land use on global change processes (Steffen et al. 2015; Erb et al. 2013; Kuemmerle et al. 2013). A very basic and fundamental research challenge is that both, socio-economic drivers, i.e. land use, as well as climatic drivers influence climatic and ecosystem changes at various scales and it is difficult to disentangle the effects of both. This is also a major challenge (and indeed the focus of WP6 and WP7) in the BACI-project, where appropriate analytical tools are required to distinguish socio-economic from climatic drivers of biosphere-atmosphere changes.

One intricacy in capturing effects of land use and land use intensity is the limited usability of remote sensing techniques, particularly when it comes to capturing effects that are beyond changes in land cover. This is related to the complex and multi-dimensional nature of land use intensity, which encompasses not only one, but three different interrelated processes (Erb et al. 2013; Kuemmerle et al. 2013): (a) inputs into the land, such as labour, fertilizer, water, nutrients, mechanization), (b) their respective outputs from the land, such as land-based products (biomass harvest), as well as (c) changes at the system level related to land use, or unintended consequences respectively, such as ecosystem degradation, carbon stock losses of biodiversity loss.

Deliverable 7.2: Rationale and research objectives

WP7 of the BACI project focuses on the socio-economic dimension of biosphere-atmosphere changes. Deliverable 7.2 aims to analyse trajectories of land use and land use intensity at the global scale in a long-term perspective. This report represents the results of deliverable 7.2., which is described as: "Report on global demand and for land-based products, and inputs in the land system in decadal time series at the global level." (from the BACI project-proposal).

As an analytical framework, we apply the "Human Appropriation of Net Primary Production" (HANPP)-framework that has gained momentum as a tool to assess the human domination of terrestrial ecosystems caused by land use. Specifically, we aim at quantifying and analysing global HANPP flows from 1910 to 2005 in a spatially explicit way. Our research goal is to trace the human impact on ecological NPP flows and to scrutinize land-use changes, i.e. land cover and land-use intensity changes, as a pressure indicator for BACI in a wall-to-wall representation (i.e. considering all occurring land use types, or 100% of each grid cell respectively).

The long-term focus allows us to a) put recent developments that are directly relevant for other BACI-working packages (i.e. the period from 2000 onwards), into perspective with historical changes of land-use impacts, in order to grasp the magnitude of recent changes, b) analyse and disentangle effects of archetypical processes, such as land use intensification versus land cover changes on NPP flows in order to understand and contrast their relevance, and c) observe land use processes in a time period for which no remote sensing data exists (before the 1970s), but which, due to past legacies, still influences todays land-use patterns. Our results will be particularly relevant for BACI, because they introduce a level of dimension that is not measurable by earth-observation/ remote sensing techniques: The level of land management, such as amounts of biomass harvest, crop yield trends and land based inputs that are largely dependent on human decision making, technological progress, economic and political frameworks, as well as on the global biomass market and international trade relations.

HANPP as an analytical framework

The ''human appropriation of net primary production'' or HANPP (Vitousek et al. 1997; Haberl et al. 2007) represents an indicator for anthropogenic land-use intensity and provides a framework for analysing the pressure exerted on terrestrial ecosystems by land use (Haberl et al. 2014). It builds upon assessments of the human interference with net primary production. Net primary production (NPP) is the annual production of biomass by primary producers (mainly plants) available for heterotrophic processes in ecosystems. HANPP measures the effects of land conversions and biomass harvest on NPP and, by integrating metrics of output intensity and system-level changes (in this case, changes in NPP_{pot}), allows us to disentangle effects of changes in land cover and land-use intensity on ecosystem energetics (Erb et al. 2009, 2013; Kuemmerle et al. 2013).

HANPP is particularly valuable in the BACI-context, because it allows neutralizing climatic factors and highlighting the role of land use on terrestrial NPP flows (refer to chapter 3.1). NPP, or carbon flows respectively, are used as the unit of measurement. Since NPP flows are directly related to many other ecosystem parameters, such as biodiversity, the water cycle, or carbon stocks, the human alteration of NPP flows allows for a proxy of changes in such parameters related to land use (Haberl et al. 2014).

Following Haberl et al. 2007 we define HANPP as the sum of two processes: A) biomass harvest through agriculture, forestry and livestock grazing ($HANPP_{harv}$) and B) indirect NPP appropriation through land cover change, such as it is the case when i.e. a natural forest is replaces by cropland or artificial pasture land ($HANPP_{luc}$). Hence, HANPP can be expressed through the following formulas:

$$HANPP = HANPP_{harv} + HANPP_{luc} \quad \text{(Equation 1)}$$

where

$$HANPP_{luc} = NPP_{pot} - NPP_{act} \quad \text{(Equation 2)}$$

NPP_{pot} represents the natural NPP level, i.e. the NPP that would occur in the ecosystem without human land use and NPP_{act} represents actual NPP, i.e. the currently prevailing NPP as the combined NPP of all occurring land use classes (agriculture, forestry, infrastructure, livestock production).

Previous work

While global HANPP maps for one time step (Haberl et al. 2007), long-term trajectories of global HANPP (Krausmann et al. 2013), as well as national and regional HANPP studies (Kastner 2009; Musel 2009; Krausmann et al. 2012; Niedertscheider et al. 2012; Niedertscheider and Erb 2014; Niedertscheider et al. 2014; Gingrich et al. 2015; Plutzar et al. 2015) are increasingly becoming available, assessments of HANPP time series at finer resolutions over large areas are lacking due to missing fine-scale input data. Fine resolution HANPP datasets covering a greater time period, however, would provide crucial information for in-depth analysis of place-specific ecological impacts of land use (e.g. on biodiversity).

This study is methodologically based on two already existing studies on global HANPP flows: Haberl et al. (2007) have calculated HANPP at a 5min resolution at the global level around the year 2000 using spatially explicit land cover and land use information for the respective year, revealing a global level of 24% of NPP appropriation from potentially available NPP (NPP_{pot}). Krausmann et al. (2013) have analysed global HANPP flows from 1910 to 2005 in a decadal time series at the national level and have shown that HANPP has doubled in the 21st century.

2. Materials and methods

We calculate HANPP trajectories in a decadal time series from 1910 to 2005 on a global level at 5 minutes resolution. We combine a set of the currently best available, spatially explicit land cover/-use data sets with historical (mostly census) data on biomass harvest, as well as with model outputs for NPP_{pot}. We follow a closed budget approach, i.e. considering 100% of each grid cell globally by quantifying land cover/-use trends of all occurring land-use types, such as cropland, forest land, grazing land and settlement areas. Unused and unproductive areas, such as permanent hot and cold deserts, are not assumed to have any effect on HANPP and are thus excluded from our calculation. The following subsections describe all data sets and methods used in more detail.

Land-use data set

As a basis of all following steps, we compiled a historic land-cover data set by evaluating available data sets in terms of their quality and usability for our HANPP database. We applied different approaches using a combination of different data sets for all considered land use-types. For croplands consistency with national data given in Krausmann et al. (2013) was considered authoritative, as these data sets are based on historical statistical records, as well as on FAOSTAT data after 1961 (FAO 2017). We used the constant 2000 national borders for downscaling statistical data into the grid. Krausmann et al. (2013) base their calculation at the level of eleven world regions, but, whenever available, also provide data at the national level. Particularly before 1961 national data was often not available and we had to deal with changing national territories. The following approach was used to model national data for such cases: We subtracted the sum of available country-level data from the regional data in order to get the sum of croplands to be redistributed to countries were data was lacking, or country borders had been changing. We used the relative share of countries with no data to the sum of cropland areas for all countries with lacking data in 1960 (refers to the year 1961), the first year with complete national cropland data. This share was considered constant in the years 1910, 1930 and 1950.

Fallow land was calculated by subtracting cropped areas from arable land. Data on arable land was taken from Krausmann et al. (2013). As mentioned, historical statistics were incomplete for the years 1910, 1930 and 1950. In case of lacking data on arable land we used the share of fallow land to cropped areas of the next available time-step. For Germany (1910) and Italy (1910, 1930, 1950) we used data from previous national studies (Niedertscheider et al. 2014; Niedertscheider and Erb 2014). For the former Soviet Union (FSU) Krausmann et al. (2013) reported regional data for the entire time-period. Hence, we used FAOSTAT data from 1992 in order to calculate the cropland share of each country belonging to the former-FSU. We considered this share constant for the entire time-period.

For the spatial allocation of national cropland areas to the grid we followed the patterns of HYDE 3.2 (Klein Goldewijk 2016). In cases where Krausmann et al. (2013) data were higher than the national aggregation of cropland pixels in HYDE 3.2, we increased the fractional covers of all cropland pixels in order to reproduce the Krausmann et al. (2013) national sums.

Grazing land was also taken from HYDE 3.2., where grazing land is defined as the sum of pasture land (potential forest land converted to grazing land) and rangeland (potential non-forest land converted to grazing land). Settlement areas were also taken from HYDE 3.2, however, as this data does not consider rural infrastructure areas, we considered that each cropland pixel contains a certain amount of rural infrastructure (3% of cropland area in 1910 linearly increasing to 5% in 2005). Wilderness areas (i.e. areas without land use) were also taken from the Hyde 3.2 dataset which also provides an "re-classification of HYDE 3.2.000 according to the Ellis and Ramankutty (2008) scheme of "Anthropogenic Biomes" or "Anthromes". The remaining areas were defined as either as *forests and woodlands* or *other land maybe grazed*. Forests and woodlands were considered in those pixels that were classified as potential forests in a map of potential vegetation (Ramankutty and Foley 1999). All other pixels are considered other land maybe grazed. Additionally, on pixels classified as village land in the HYDE "Anthromes" data (Ellis and Ramankutty 2008) 90% of the hitherto unclassified land were defined as other land maybe grazed, while 10% were considered forest land. This approach was chosen in order to account for the proximity of more intensively used land classes, such as pasture land, to villages and infrastructure areas.

$HANPP_{harv}$: Biomass harvest

Biomass harvest on croplands, forest land and grazing land were taken from Krausmann et al. (2013). We used the same approach as described above for the land use/-cover data set for modelling biomass harvest in the case of changing country borders or lacking national data in the pre-1961 period, as well as for the former FSU countries.

In our definition $HANPP_{harv}$ does not only contain the merchantable part of a plant that is usually reported in statistical records (i.e. timber, fuelwood, primary crop harvest), but also contains used and unused residues, such as felling losses and crop by-products, i.e. straw. The detailed methods for extrapolating primary harvest to $HANPP_{harv}$ are described in the supplementary material of Krausmann et al. (2013). Basically, harvest factors that account for by-products were based on literature recherché in order to integrate industrialization and technological change as factors that have decreased the share of by-products to the total plant. This was particularly relevant for cropland production in Europe, the North America and Eastern Asia from the post-World War II period onwards, when new agricultural technologies of the so-called "Green Revolution" allowed for drastically increasing biomass yields (Krausmann et al. 2013).

Cropland harvest was spatially downscaled to the HYDE 3.2 cropland patterns following an index created through the combination of NPP_{pot} patterns with patterns of irrigated land (HYDE 3.2. based on Siebert et al. 2015). Hence, we assumed that cropland yields were higher in regions of high NPP_{pot}, where temperature and water availability are usually favourable for agricultural production, as well as on irrigated land, where aridity is counterbalanced through external water inputs (Niedertscheider et al. 2016b; Smith et al. 2014c).

No data on spatially explicit forest harvest exists, which is why we assumed forestry harvest to follow the patterns of forest NPP_{pot}. However, we excluded areas that were defined as “wilderness” in Sandersen et al. (2009). Harvest on grazing land was calculated based on feed demand values, which were calculated through livestock numbers using the methods for different animal species described in Krausmann et al. 2013.

Harvest on grazing land was downscaled to the grid following the HYDE 3.2 patterns of grazing land. Two basic considerations were important here:

1. The fraction of NPP_{act} on grazing land that is available for grazers had to be defined. On grazing land pixels that belong to pasture land in HYDE 3.2, the entire aboveground fraction (50% of total NPP; Haberl et al. 2007) was considered accessible for grazers, while on rangeland and other land may be grazed a certain fraction was assumed to be covered by woody vegetation and thus was excluded from grazing, i.e. in the case of savannahs, or shrublands. Here, we used values provided by Fetzel et al. (2017), who provide the following factors for aboveground NPP:

- natural grasslands: 100%
- other wooded land: 70%

These factors were spatially joined with three different biome maps (Ramankutty and Foley 1999; Olson et al. 2001; Simons et al. 2001), where the mean factor between the maps was taken as a multiplier for NPP_{act} in each pixel.

2. For the allocation of grazed biomass into the grid, we additionally followed a grazing-intensity function assuming that regions of high NPP_{act} are over-proportionally grazed compared to regions of lower NPP_{act}.

Actual NPP (NPP_{act})

Actual cropland NPP was extrapolated from cropland $HANPP_{harv}$ using country-specific pre-harvest loss factors. These factors were taken from Krausmann et al. (2013) and are temporally dynamic in order to account for a decrease of NPP losses in the course of industrialization. In line with common practice in HANPP studies, NPP_{act} on forest land was assumed to equal NPP_{pot} and NPP_{act} on infrastructure land was considered to be one third of NPP_{pot} assuming one third of the area carries highly productive vegetation (Haberl et al. 2014). On grazing land located on potential forest land 20% of NPP_{pot} were deducted to arrive at NPP_{act}. Additionally, to account for degradation on grazing land, deduction factors derived from Zika and Erb (2009) were applied. In the present version, the low estimate was used to arrive at conservative results.

Potential NPP (NPP_{pot}) and HANPP

Potential NPP (NPP_{pot}) trends were calculated by the Lund-Potsdam-Jena Global Dynamic Vegetation Model. Several LPJ-runs exist, where we use the version in Krausmann et al (2013) in order to warrant the highest possible level of consistency. HANPP was finally calculated as the sum of $HANPP_{harv}$ and $HANPP_{luc}$ (defined as the difference between NPP_{pot} and NPP_{act}).

In order to assess the influence and potential uncertainty of our results due to the model-derived NPP_{pot}, we contrasted our results with an alternative HANPP calculation applying outputs of a different DGVM: LPJ-GUESS (Smith et al. 2001, 2014a).

External drivers of HANPP: IPAT

In order to highlight the effects of external drivers on HANPP patterns, we calculated the correlation between HANPP patterns and patterns of inputs of nitrogen (Lu and Tian 2017), irrigation (Klein Goldewijk 2016; which uses data from Siebert et al. 2015), population (Klein Goldewijk 2016) and GDP (Nordhaus 2005; Nordhaus and Chen 2016). This allows us to integrate the "input" dimension of land use into our analysis, which is a priori not integrated in the HANPP framework. The external drivers analysed here resemble the input variables of the IPAT-model (Ehrlich and Holdren 1971; Commoner 1972), which attributes a certain impact (I), in our case HANPP changes, to respective drivers, i.e. population changes (P), affluence approximated by GDP changes (A) and technology, expressed by changes in nitrogen and irrigation (T). We focus on IPAT changes between 2000 and 2005, as this is the period most relevant for other BACI working packages. The IPAT approach allows us to highlight the relevance of the mentioned input-parameters on changes in HANPP flows. This information is crucial when interpreting past HANPP patterns, but it is also helpful for grasping possible future land-use impacts of different socio-economic pathways in terms of demographic change, economic development and technological change.

3. Hundred years of land use change

Overall HANPP trajectories in the past 100 years

In the course of the 20th century global NPP appropriation measured by the HANPP indicator framework, has doubled from 6.5 billion tons carbon (bio t C) in 1910 to 12.9 bio tC in 2005 (Figure 1A; refer also to Krausmann et al. 2013). Expressed as a share of natural NPP (NPP_{pot}) the HANPP increase was less drastic, i.e. increasing from 13% to 22% in the observed period (Figure 1B). This is related to potential NPP, which showed a steady rise from 51.8 bio tC to 59.1 bio tC between 1910 and 2005 (Figure 1A secondary axis), owing to climatic changes, increasing N-availability and rising CO_2 levels in the atmosphere (Sitch et al. 2003a). Our HANPP results (Figure 1) are slightly lower than the results in Krausmann et al. (2013), which owes to the spatially explicit calculation of HANPP and its indicators that allows for the more fine-scale representation of land use impacts, taking into account also local to regional ecosystem properties.

HANPP dynamics were strikingly different in the eleven world regions analysed here (Figure 1). The world regions correspond to the regions analysed in Krausmann et al. (2013). While Western Europe has revealed continuously decreasing HANPP % NPP_{pot} since the beginning of the observed time period, Northern Africa and Western Asia, Eastern and South-Eastern Europe, Oceania and Australia, as well as Central Asia and Russian Federation witnessed a turning point from increasing to decreasing HANPP in the 1980s and 1990s (Figure 1B, also refer to the appendix figures A2 to A4). The most prominent increase of HANPP has occurred in world regions that revealed low to moderate levels of HANPP throughout the time period: In Latin America and the Carribbean, South-East Asia, Sub-Saharan Africa and Eastern Asia, HANPP % NPP_{pot} has been rising by 227%, 136%, 133% and 110% since 1910 (Figure 1B). The tabular trends presented in Figure 1 are supported by the respective global maps on HANPP trajectories, which can be found in the Appendix (Figures A2 to A4) for the years 1910, 1950, 1980, 2000 and 2005.

Our findings resemble the archetypical HANPP patterns described in previous studies (Jepsen et al. 2015; Gingrich et al. 2015; Krausmann et al. 2012; Kastner 2009): HANPP starts at low levels and usually increases owing to population growth and resulting land expansion under relatively low biomass yields. In the course of industrialization followed by intensification of agriculture, HANPP stabilizes at high levels, as biomass demands are not satisfied by expanding agricultural areas, but by increasing outputs per area (also refer to the seminal study by Boserup 1965). In highly industrialized regions, HANPP even declines, as forests grow back on abandoned, mostly marginal agricultural areas. This process is termed “forest transition” in the literature and was observed for many Western European countries, as well as in parts of the US and Southeast Asia (Mather 2001; Rudel et al. 2005; Meyfroidt and Lambin 2011).

Hence, unsurprisingly, the trends towards increasing HANPP in some world regions is chiefly found in the developing world, where land expansion is still the dominating land use trend, whereas input-output intensification levels are commonly low (Niedertscheider et al. 2016b; Fetzel et al. 2016) . These findings are also mirrored in terms of biomass harvest trends ($HANPP_{harv}$) and particularly in the trends of HANPP efficiency (calculated as the share of $HANPP_{harv}$ to HANPP), which show striking difference between the world regions (Figure 1C D). Globally, total biomass harvest increased even more drastic than HANPP, revealing an almost threefold increase from 3.1 bio tC in 1910 to around 9.0 bio tC in 2005 (Figure 1C). As a consequence, HANPP efficiency has improved greatly. While in 1910 only 48% of HANPP consisted of $HANPP_{harv}$, this share grew to 70% in 2005 (Figure 1D).

HANPP efficiency reached levels above 100% in Southern Asia, Northern Africa and Western Asia from 1990 onwards. This can be explained by land management that was responsible for actual NPP (NPP_{act}) to surpass potential NPP (NPP_{pot}), resulting in negative $HANPP_{luc}$. In Eastern Asia HANPP efficiency above 100% was even the case from 1970 onwards. These trends are directly related to output intensification, along which levels of harvest per area increase and NPP_{act} rises at the cost of $HANPP_{luc}$, indicating that the NPP losses associated with land use are declining. Vice versa, low levels of HANPP efficiency indicate low levels of output intensification. This was the case particularly in Sub-Saharan Africa and Central Asia and Russian Federation, where only 40 and 48% of HANPP entered the socio-economic system in the form of harvest, while the remaining part ($HANPP_{luc}$) and the lion's share was lost in the course of land conversion. Other studies come to similar conclusions in terms of low levels of land-use intensity that is related to a historical reliance on land expansion as a way to increase biomass harvest in order to cope with population growth in many parts of Sub-Saharan Africa (Niedertscheider et al. 2016a; Bartels 2013; Fetzel et al. 2016).

While the contribution to total HANPP in 2005 was dominated by Latin America and the Carribean, Northern America and Sub-Saharan Africa, the contribution to total biomass harvest ($HANPP_{harv}$) was dominated by Latin America and the Carribean, Eastern Asia, Southeast Asia and North America. Sub-Saharan Africa contributed only 11% to global $HANPP_{harv}$.

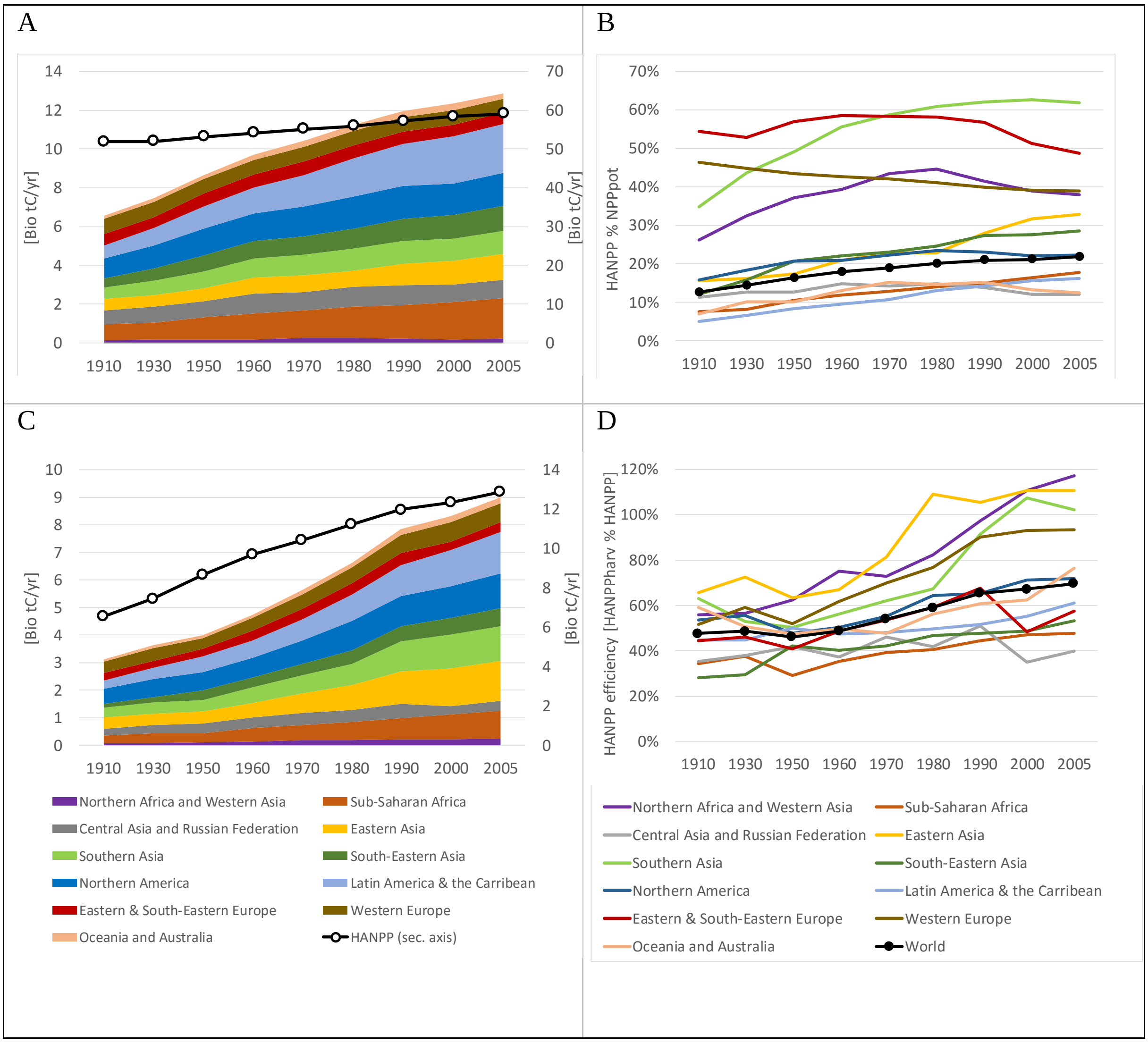

Figure 1: HANPP trends from 1910 to 2005 broken down to eleven world regions. A) Regional totals in Billions tons Carbon per year [bio tC/yr]; the secondary axis depicts the NPP_{pot} trend. B) HANPP as percentage of NPP_{pot} globally (dotted line) and for the world regions. C) biomass harvest ($HANPP_{harv}$) broken down to the world regions, with the HANPP-trend on the secondary axis. D) share of $HANPP_{harv}$ per unit of HANPP as a proxy for HANPP efficiency. Colour codes of A, B, C and D match.

HANPP patterns in 2005

Figure 2 reveals the global patterns of HANPP (A) and $HANPP_{harv}$ (B) in 2005. HANPP was distributed extremely uneven across the globe, where high levels (between 300 and 400 gC/m2/yr) are particularly found in central and eastern Europe, the US, Southern Brazil, India, Nigeria and Eastern China (Figure 2A, B). Harvested NPP ($HANPP_{harv}$) resembles HANPP patterns relatively closely. However, here Northern Europe and Eastern China, as well as parts of North-East India turn out as hotpots, whereas South America, the US and Nigeria show lower levels compared to their HANPP patterns, supporting the previous paragraphs, where HANPP efficiency had been described as low in many African parts and high in Southeast Asia and Southern Asia. Eastern European and Sub-Saharan African countries reveal very low levels of $HANPP_{harv}$. $HANPP_{harv}$ was generally higher in regions dominated by croplands (refer to the appendix Figures A2 and A3) that are usually more intensively managed, as are grazing lands in many parts of the world. Population density is an additional factor that promotes high HANPP and $HANPP_{harv}$ levels. The US, for instance is a highly industrialized country, but, owing to the low population pressure, reveals lower $HANPP_{harv}$ levels as compared to, for instance Europe, or Eastern China. Naturally, climatic and topographic factors are pivotal drivers of the dominant land-use type in a pixel, where the more arid regions follow a gradient towards higher specialization on grazing, which is commonly managed less intensively as compared to croplands, corresponding in lower $HANPP_{harv}$.

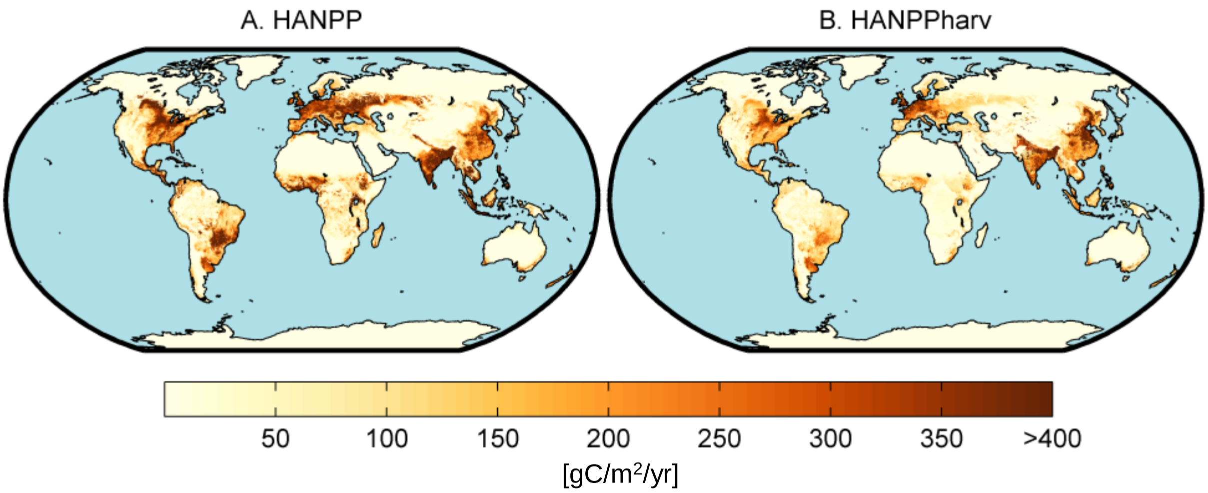

Figure 2: HANPP flows in the year 2005. A HANPP and B $HANPP_{harv}$ in $gC/m^2/yr$.

In 2005 human land use has decreased NPP_{pot} by roughly 7% (i.e. $HANPP_{luc}$ = 7% of NPP_{pot}). In other words, NPP_{act} amounted to 93% of NPP_{pot} in 2005 (Figure 3 A, B), of which approximately 13% were extracted through harvest (Figure 2B). HANPP patterns described above do not strictly follow patterns of NPP_{act} and NPP_{pot} (Figure 3 A, B) in most world regions. Particularly the tropical countries of Africa, Southeast Asia and South America reveal the highest NPP_{pot} levels of above 1000 gC/m2/yr, while their HANPP levels were rather low. Exceptions are those areas of the tropics, where agriculture has developed as the predominant land use form over the past decades (refer to Figures A3), leading to a high HANPP and NPP_{act} lower than NPP_{pot}. Examples are the soy-growing regions of Southern Brazil, or the tropical parts of Western Africa, i.e. along the Gulf of Guinea, as well as parts of the Congo basin. In these regions agriculture has replaced areas of high NPP_{pot}, leading to the highest $HANPP_{luc}$ levels globally (Niedertscheider et al. 2016b). NPP_{act} was also drastically lower than NPP_{pot} in regions of the former Soviet Union, where high shares of NPP_{pot} were lost, supporting previous research that has revealed low output-intensity together with high system level impacts (Niedertscheider et al. 2016b).

In Western Europe, the Iberian Penisula stands out as a region where NPP_{act} was significantly lower than NPP_{pot}, while the remaining areas of this region show only moderate differences between NPP_{pot} and NPP_{act}. Spain is also prone to high HANPP combined with relatively low $HANPP_{harv}$ in the regional context. A few parts of the world reveal higher NPP_{act} than NPP_{pot}. These regions are mainly situated in the agricultural dry-land regions, where particularly irrigation and intensive land management allows for NPP_{act} to surpass NPP_{pot} (Siebert et al. 2015). Examples are the Indus region of North India and Pakistan.

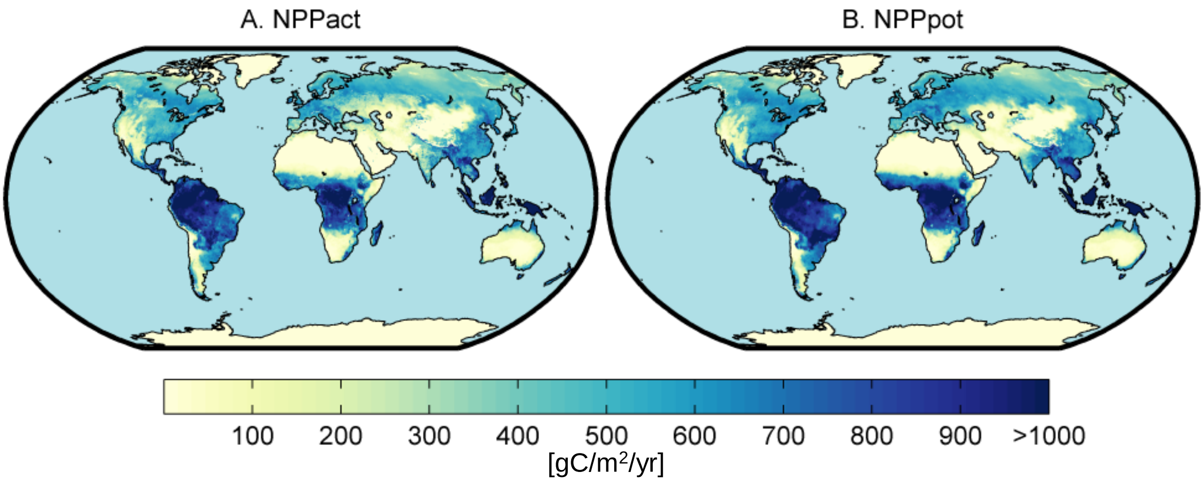

Figure 3: NPP flows in the year 2005. A actual NPP and B potential NPP in gC/m²/yr.

Comparing periods of HANPP changes: Recent developments in perspective with long-term trends

The spatially explicit HANPP results and its components are presented in the Appendix for the time-steps 1910, 1950, 1980, 2000 and 2005. As changes of land use will be particularly important in the BACI context (BACI is, by definition, a change indicator), we will focus on changes of HANPP and its indicators for different sub-periods in the following sub-chapters. Figure 4 to Figure 14 represent the changes of land cover, HANPP and its indicators between 1910 and 1960 (A), 1960 to 2005 (B), 1910-2005 (C) and for 2000 to 2005 (D), which is also the period in which most BACI downstream products will become available. Hence, for the BACI-context and the empirical parts of related WPs, panels D might be most suitable for direct use, such as for validation of the BACI-index and the downstream products (WP6). Panels A,B and C allow to put recent changes (D) into perspective with historical changes in order to get an impression on their magnitude in the temporal context.

Land cover changes were drastic since 1910 and did not follow uniform patterns across the world (Figure 4- Figure 7). A striking gradient between industrialized Europe and the developing world appears in terms of cropland trajectories. Globally, croplands increased from ca. 9 Bio km^2 in 1910 to more 15.4 Bio km^2 in 2005, which corresponds to a 70% increase. Western and Northern Europe experienced a continuous cropland decrease over the entire time period (Figure 4C), while the lion's share of cropland expansion occurred in Sub-Saharan Africa and Southern Asia, where croplands increased from 1910 to 2005. Different phases of initial expansion between 1910 and 1960 (Figure 4A) and decline afterwards (1960-2005, Figure 4B) are found in Eastern Europe and the former Soviet Union countries, but also in the US corn-belt. In Eastern Europe and the former Soviet Union this is related to the collapse of communism and the democratic transition in the 1990, which led to drastic institutional changes and to a sudden brake-down of the agricultural system. Agricultural abandonment was high (Prishchepov et al. 2012; Kuemmerle et al. 2011; Hostert et al. 2011; Niedertscheider et al. 2014) and only in the most recent period, croplands started to increase again in some parts (Figure 4D).

Grazing lands declined in central Europe too, which, together with the observed increase of woodland areas supports the notion of a forest transition found in the literature (Figure 5, Figure 6) (Jepsen et al. 2015; Rudel et al. 2005; Mather 2001; Meyfroidt and Lambin 2011) that follows agricultural regime shifts and a trend towards increasing biomass imports. Opposite trends of agricultural expansion at the cost of woodlands are found in the remaining world regions, particularly in South America, Southeast Asia and Sub-Saharan Africa. These global heterogeneities indicate a diversification between biomass exporting and importing regions across the past century, but chiefly in the second period (panels B), where global markets become more important and global biomass trade increased. Europe stands out a region that heavily relies on biomass imports, particularly from South America (Kastner et al. 2015). Hence, European biomass consumption has to some extent externalized related land-use impacts to distant, often developing world regions (Kastner et al. 2011, 2015). Forests also regrew in parts of the US (Figure 6 B).

Most shifts in land-cover occurred in the pre-2000 time period, while between 2000 and 2005 changes were comparably modest. However, considering the short time-span of only five years, several interesting shifts appear (Figure 4- Figure 7, panels D): Croplands revealed the greatest dynamics in this period and show expansion hotspots in Southern Brazil, Western US and below the Sahel-belt, but elsewhere witnessed declines. Argentina, Colombia, Southern Europe and Botswana appear as hotspots of cropland decline between 2000 and 2005 (Figure 4 D). Woodlands show moderate shifts, except for Eastern Europe and parts of South-Eastern China, where woodlands increased, in contrast to Eastern China and parts of the central Asia, the Ukraine and Belarus, where deforestation hotspots prevailed (Figure 6 D).

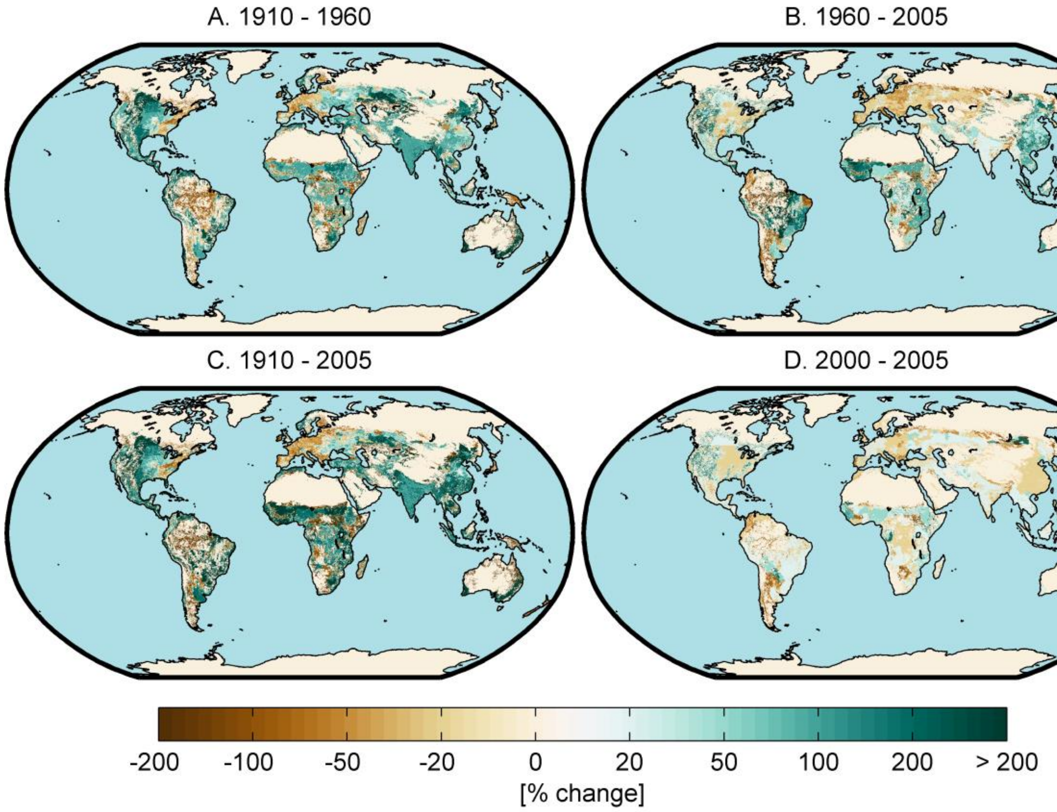

Figure 4: Changes of cropland extent in % absolute change from A 1910-1960, B 1960-2005, C. 1910-2005 and D. 2000-2005.

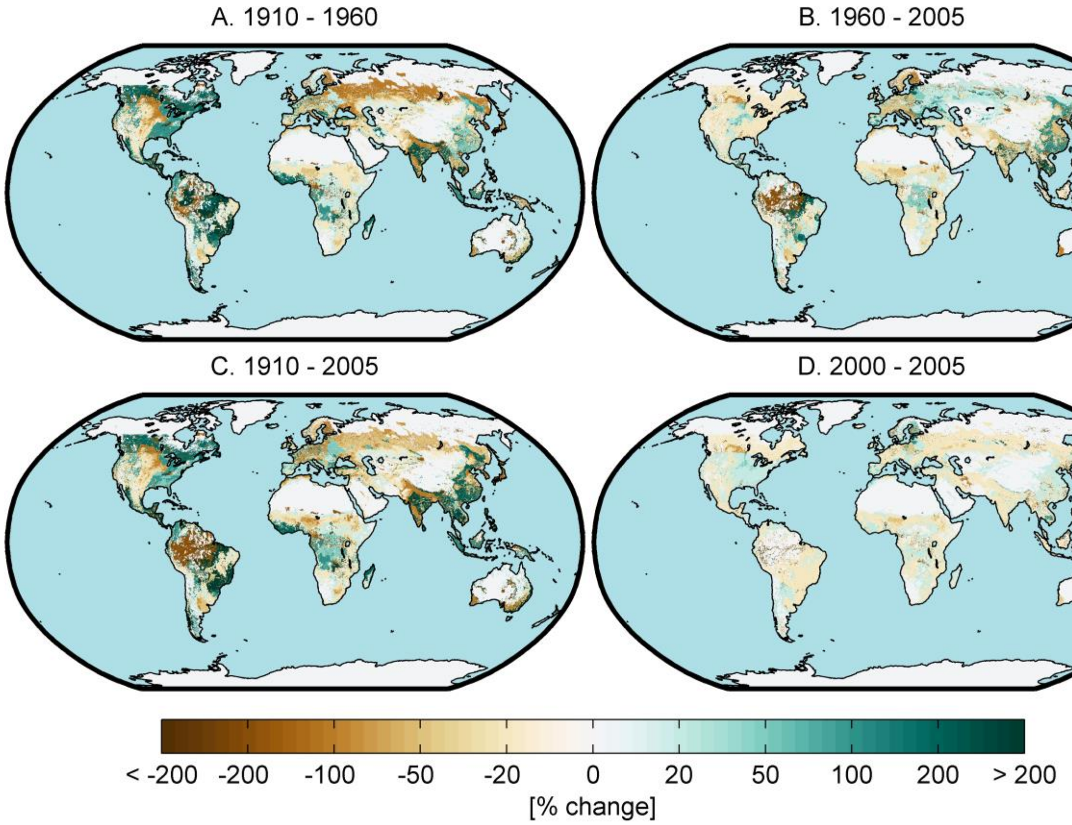

Figure 5: Changes of grazing land extent in % absolute change from A 1910-1960, B 1960-2005, C. 1910-2005 and D. 2000-2005.

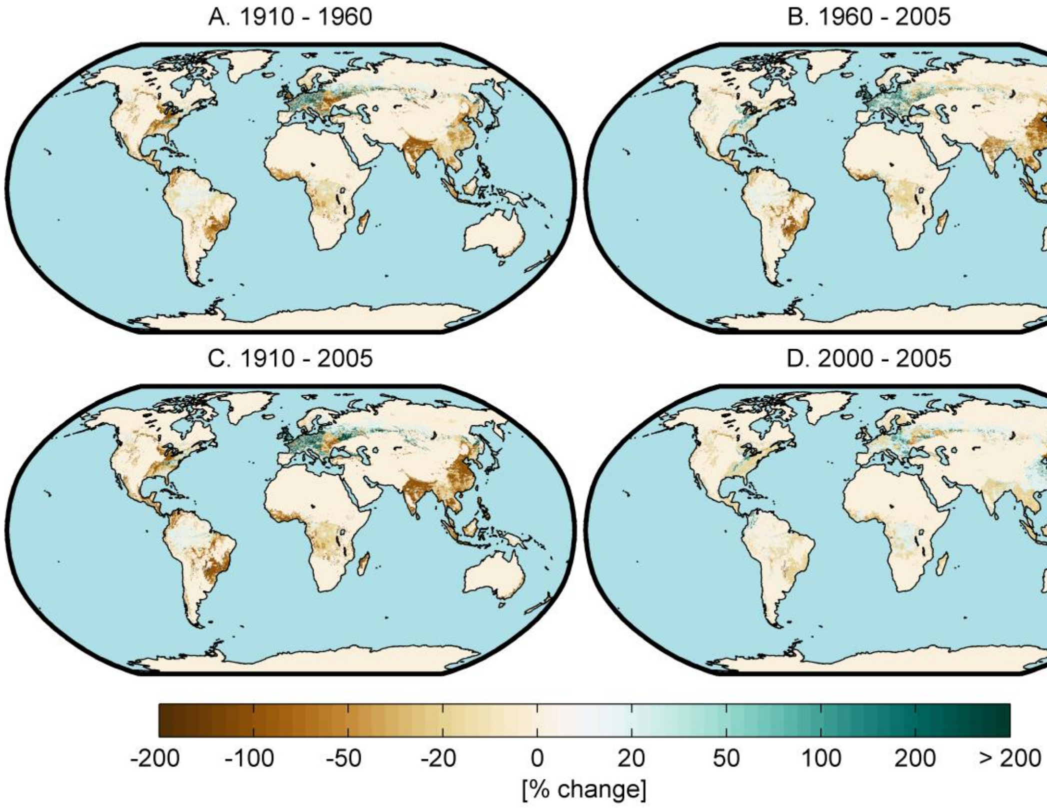

Figure 6: Changes of woodland extent in % absolute change from A 1910-1960, B 1960-2005, C. 1910-2005 and D. 2000-2005.

Build-up areas contribute low shares to the global land cover, but nevertheless increased substantially from 0.4 Bio km^2 in 1910 to 1.2 Bio km2 in 2005. Particularly the developing world of Sub-Saharan Africa, South Asia, mostly India and parts of Latin America saw drastic expansion of infrastructure areas, witnessing approximately 6-fold increases (Figure 7). Increases were lower in Europe and support the lower levels of population increases (FAO 2017; Klein Goldewijk 2016).

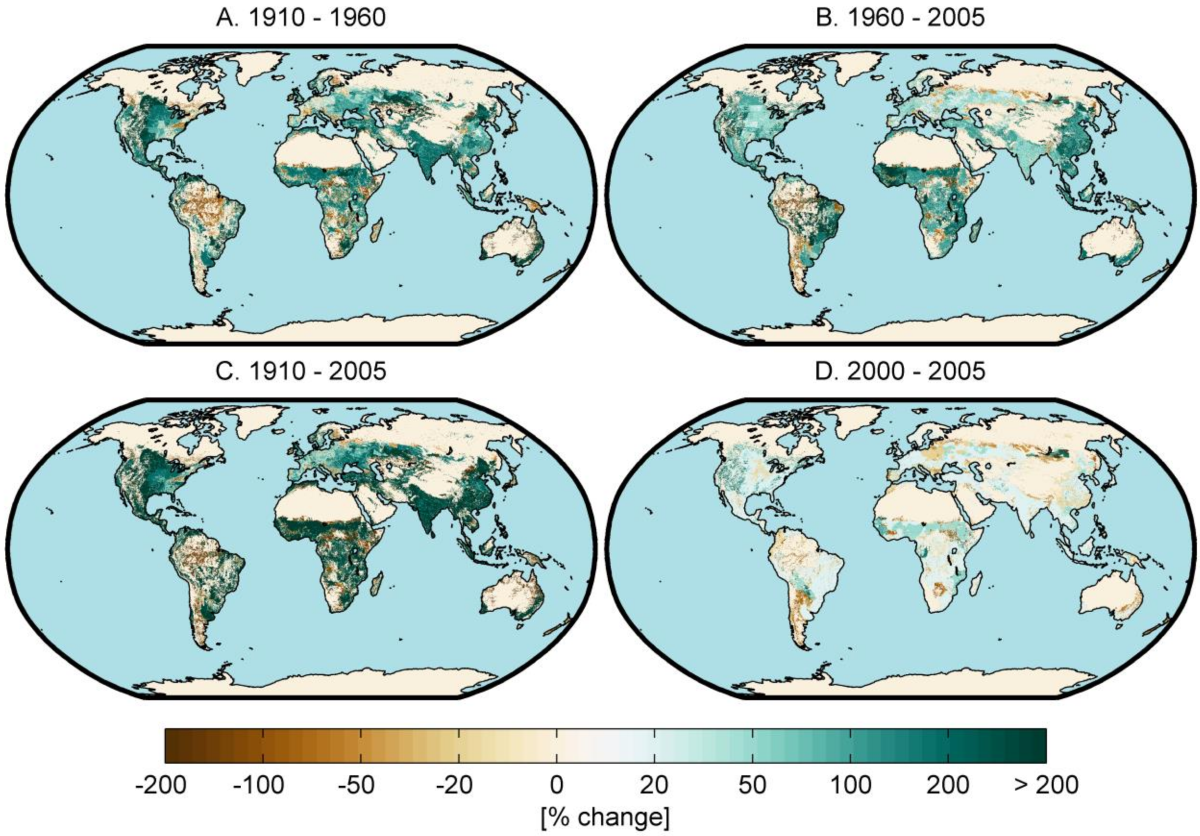

Figure 7: Changes of build-up areas in % absolute change from A 1910-1960, B 1960-2005, C. 1910-2005 and D. 2000-2005.

Again, a clear distinction between Europe and central Asia and the rest of the world can be witnessed in terms of HANPP changes, both, calculated as HANPP per area (Figure 8) and as percentage of NPP_{pot} (Figure 9), where European HANPP decreased already between 1910 and 1960, but elsewhere HANPP increased. Interestingly, European $HANPP_{harv}$ per area increased simultaneously, which supports the initial finding of high HANPP efficiency in the industrialized world. In contrast, Russia and the former Soviet Union countries experienced declining $HANPP_{harv}$ in the 1960-2005 period, which was largely a consequence of the fall of the iron curtain, which, as mentioned above, brought about a sudden collapse of the agricultural production system in most former communist countries. This was specifically experienced in the livestock sector and as a consequence grazing $HANPP_{harv}$ declined drastically (

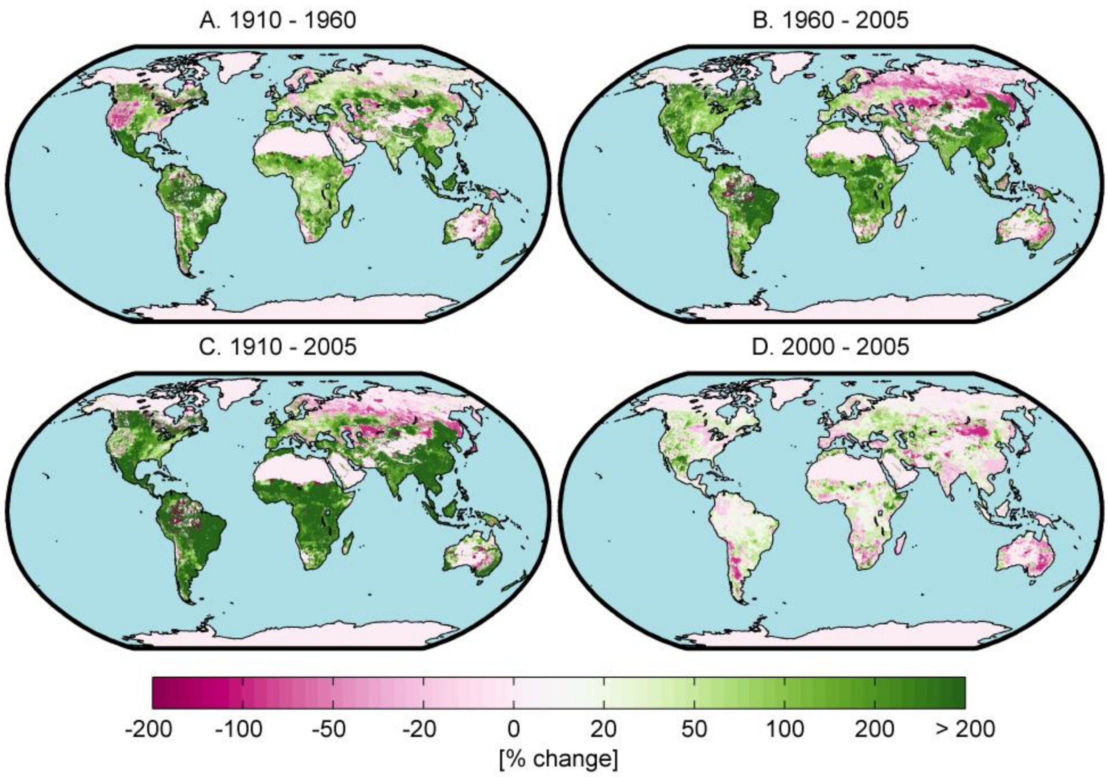

Figure *10*, Figure 9) (Kuemmerle et al. 2011; Prishchepov et al. 2012; Niedertscheider et al. 2014).

Between 2000 and 2005 HANPP changes were more dynamic when expressed as HANPP per unit area (Figure 8D), compared to HANPP % NPP_{pot} (Figure 9D). This is related to climatic factors that are neutralized when HANPP is related to NPP_{pot}, while land-use effects are highlighted. In several regions, such as Southern Argentina, or Australia, this even resulted in a different direction of change, i.e. HANPP per area declined, while HANPP % NPP_{pot} increased, as a result of declining NPP_{pot} in the same time span (refer to appendix Figure A1).

Hence, those regions that stand out as hot-or cold-spots of HANPP % of NPP_{pot} changes can be defined as hotspots of land use change. From 2000 to 2005 particularly Mongolia showed rapid decreases of HANPP % NPP_{pot} due to declining livestock numbers that was followed by declining $HANPP_{harv}$ on grazing lands (Figure 12 D), while the Indus region (N-India and Pakistan) experiences a drop in HANPP % NPP_{pot} due to rising cropland productivity (NPP_{act}; refer to appendix Figure 1A) and cropland yields (Figure 11 D).

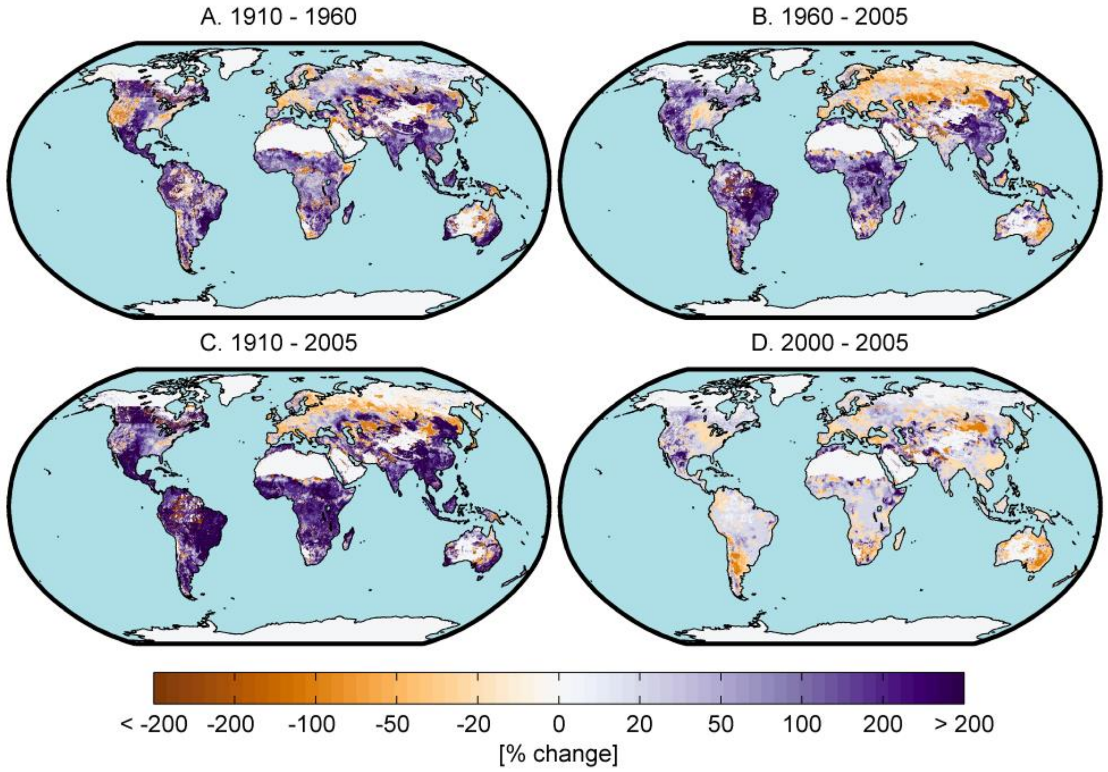

Figure 8: Changes of HANPP [gC / m2/ yr] in percent absolute change from A 1910-1960, B 1960-2005, C. 1910-2005 and D. 2000-2005.

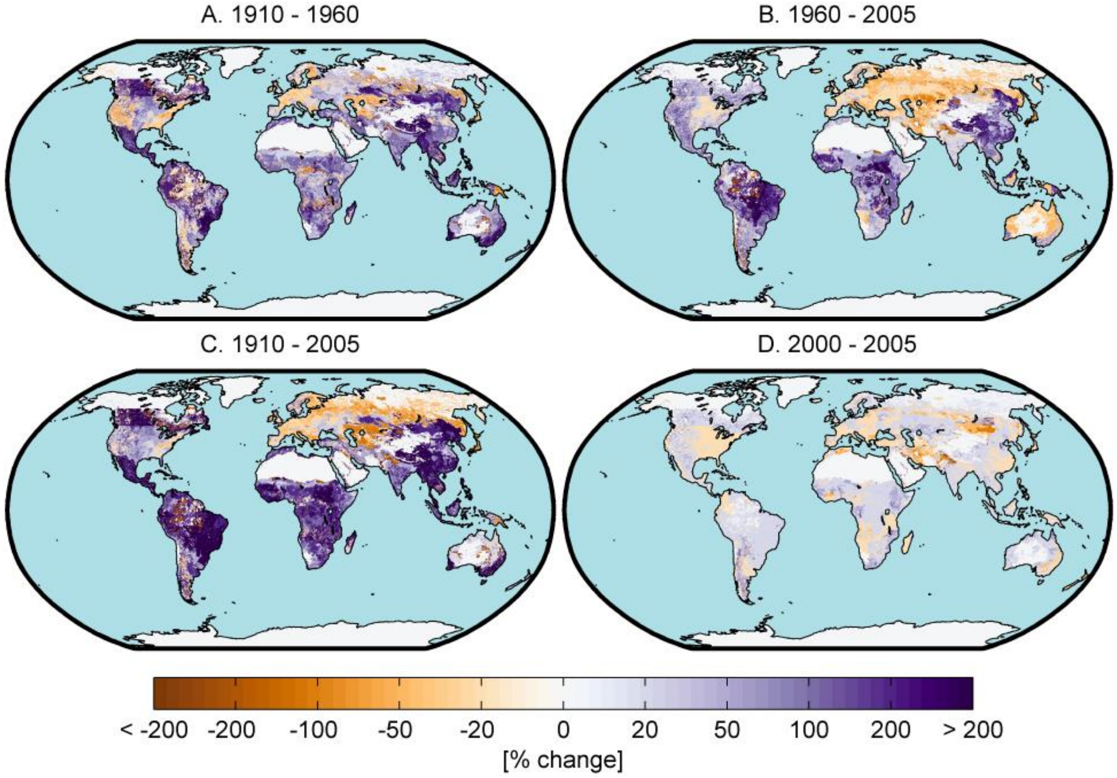

Figure 9: Changes of HANPP in % of NPP_{pot} in percent absolute change from A 1910-1960, B 1960-2005, C. 1910-2005 and D. 2000-2005.

Harvested NPP per area ($HANPP_{harv}$) increased in all world regions from 1910 to 2005, expect for Scandinavia, and parts of Russia and central Asia (Figure 10 C), which experienced a drop of $HANPP_{harv}$ particularly in the 1960 to 2005 period. Globally $HANPP_{harv}$ almost doubled since 2005, and reached a level of 12.9 Bio tons C in 2005. Latin America and Southeast Asia even saw a five-fold increase of $HANPP_{harv}$ as the combined effect of yield increases and agricultural expansion.

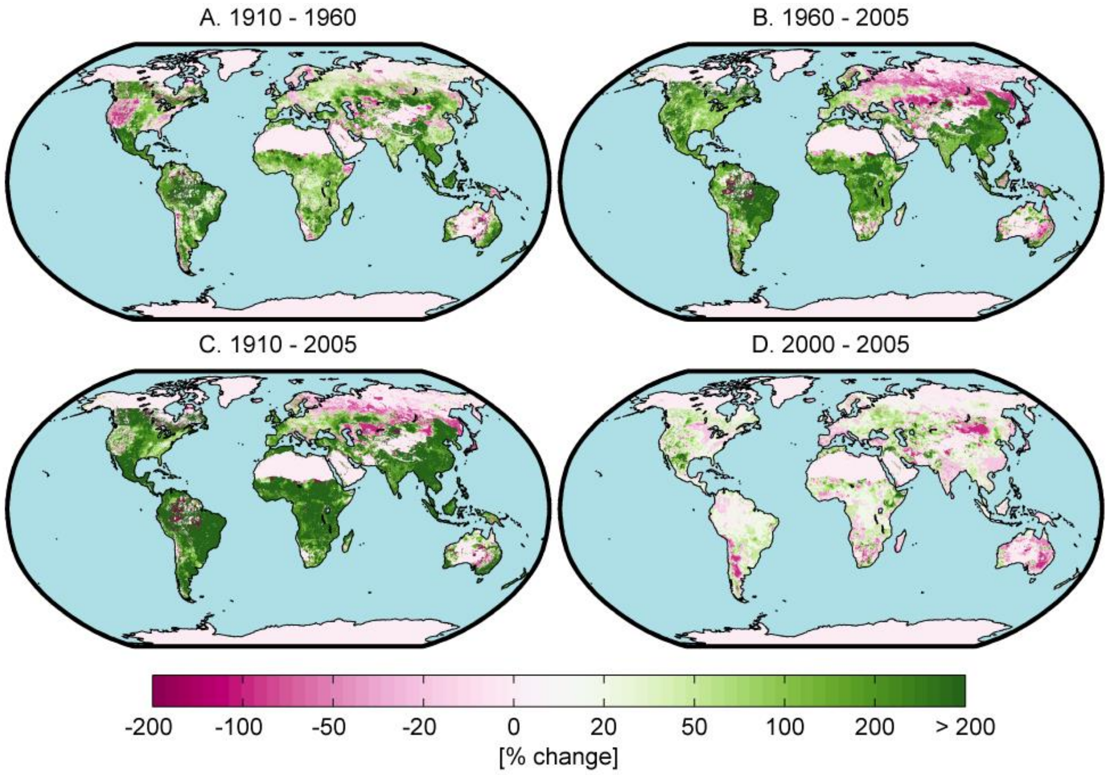

Figure 10: Changes in $HANPP_{harv}$ [gC/m2/yr] in percent absolute change from A 1910-1960, B 1960-2005, C. 1910-2005 and D. 2000-2005.

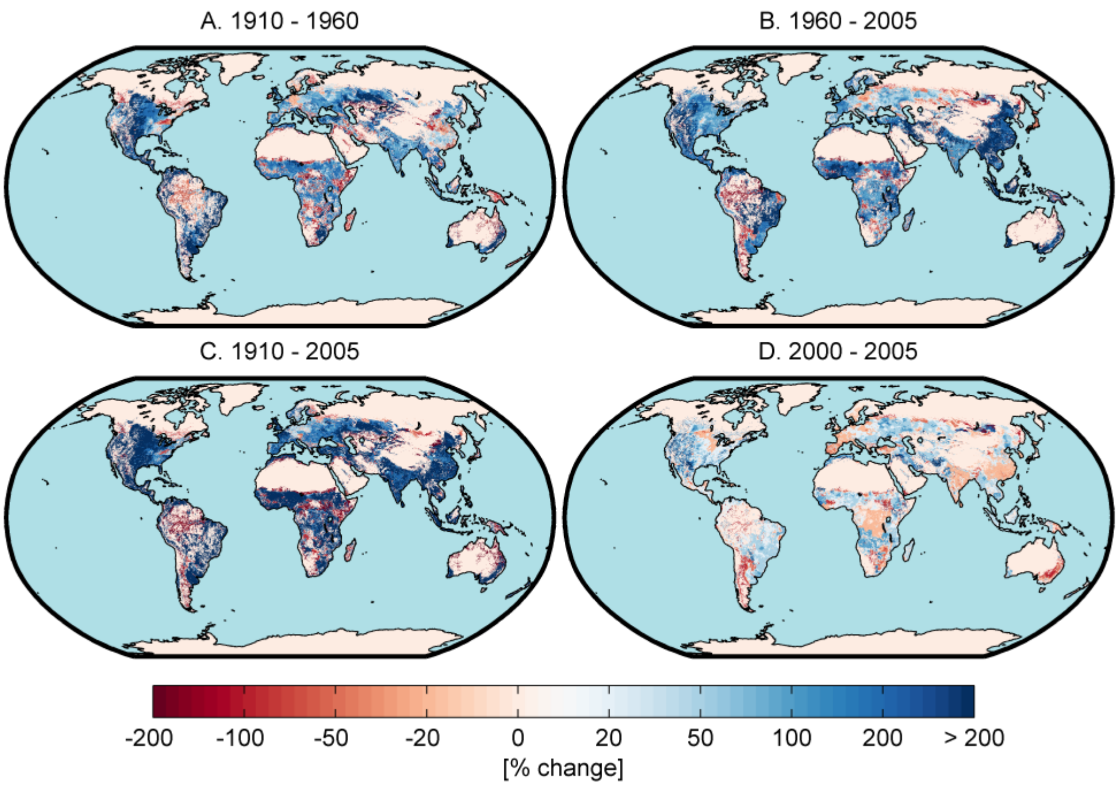

Figure 11: Changes in $HANPP_{harv}$ on croplands [gC/m2/yr] in percent absolute change from A 1910-1960, B 1960-2005, C. 1910-2005 and D. 2000-2005.

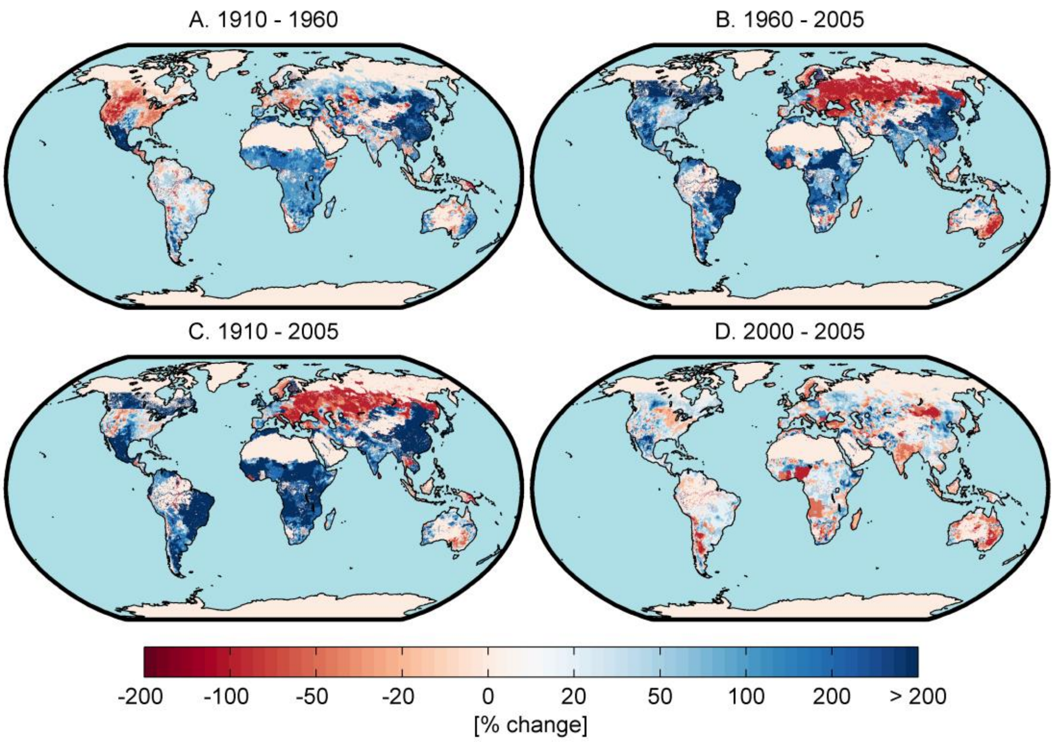

Figure 12: Changes in $HANPP_{harv}$ on grazing land [gC/m2/yr] in percent absolute change from A 1910-1960, B 1960-2005, C. 1910-2005 and D. 2000-2005.

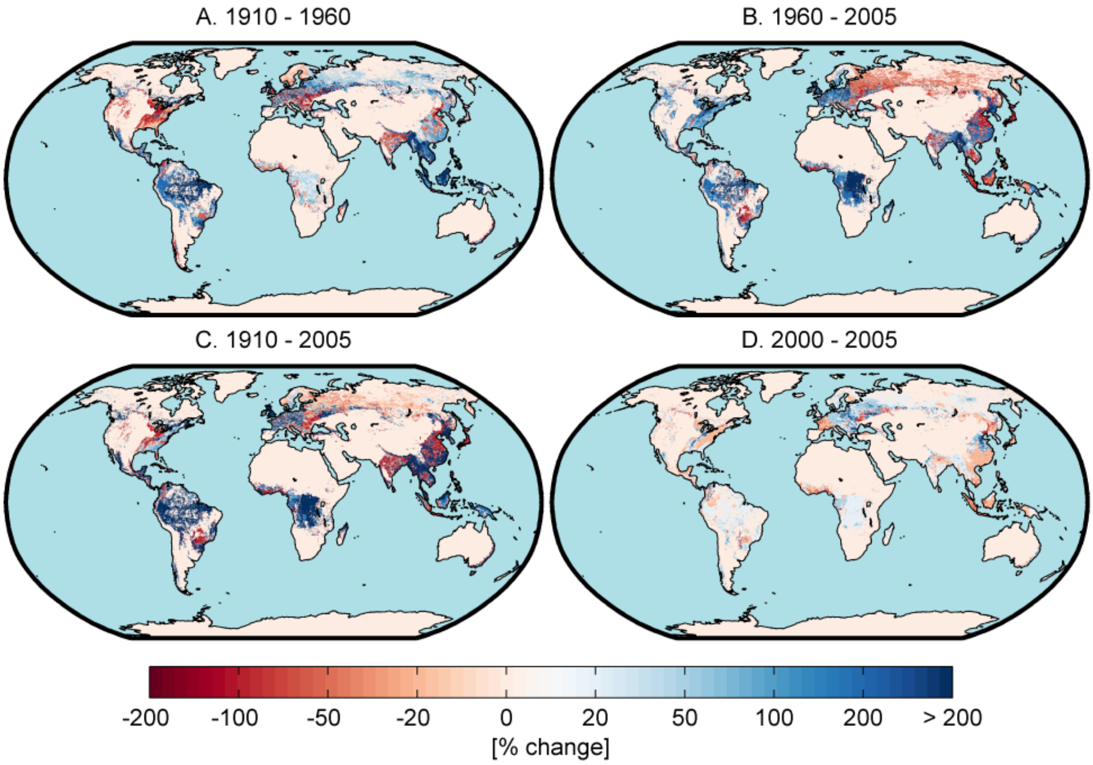

Figure 13: Changes in HANPP$_{harv}$ on forest land [gC/m2/yr] in percent absolute change from A 1910-1960, B 1960-2005, C. 1910-2005 and D. 2000-2005.

HANPP$_{luc}$ patterns indicate changes in the distance between actual and potential NPP. Declining levels indicate rising actual NPP, often a result of improved land management. This was experienced in Europe, East Asia, and parts of Latin America from 1910 to 2005 (Figure 14 C). In Sub-Saharan Africa, Brazil, Southeast Asia and Northern America HANPP$_{luc}$ increased in the past 100 years, an indication of the impacts of land conversion for agricultural production that has led to NPP losses, particularly in those regions, where initial NPP$_{pot}$ was high (Niedertscheider et al. 2016b; Smith et al. 2014c) (Figure 4, Figure 5, refer to Annex Figure A1, A2).

Hence, HANPP$_{luc}$ patterns allow for a distinction of regions that have heavily relied on agricultural expansion, from regions that relied on agricultural productivity increases in order to meet biomass demands over the past decades. The US corn-belt, China and India shifted from a period of HANPP$_{luc}$ increases (1910-1960, Figure 14 A) to a period of HANPP$_{luc}$ decreases (1960-2005, Figure 14 B) in the course of post WWII land-use intensification trends.

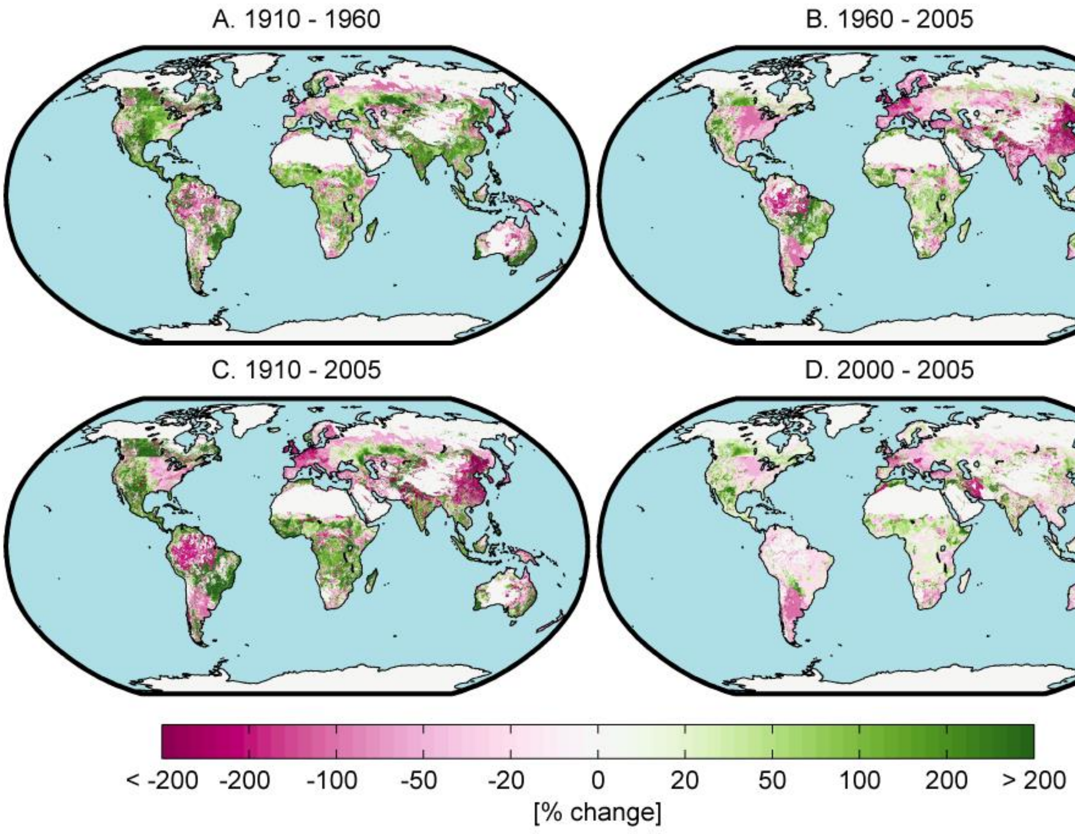

Figure 14: HANPP$_{luc}$ changes in percent absolute change from A 1910-1960, B 1960-2005, C. 1910-2005 and D. 2000-2005.

IPAT: Impacts of HANPP changes related to changes of population, affluence and technology

This chapter represents a first analysis of HANPP changes between 2000 and 2005 (Figure 16) together with changes in the related input parameters as defined in the IPAT-equation. Note that Figure 16 resembles the same input data, but a different colour-scaling as Figure 9D. HANPP decreased by more than 50% in parts of Algeria and Mongolia and Northern India. The decrease was more moderate in the US-cornbelt, parts of central Asia and North Colombia. The most drastic increases of HANPP % NPP_{pot} occurred in Sub-Saharan Africa, Southern America, as well as on the Arabic peninsula. Elsewhere HANP changes were lower, i.e. between +/- 10 to 20%.

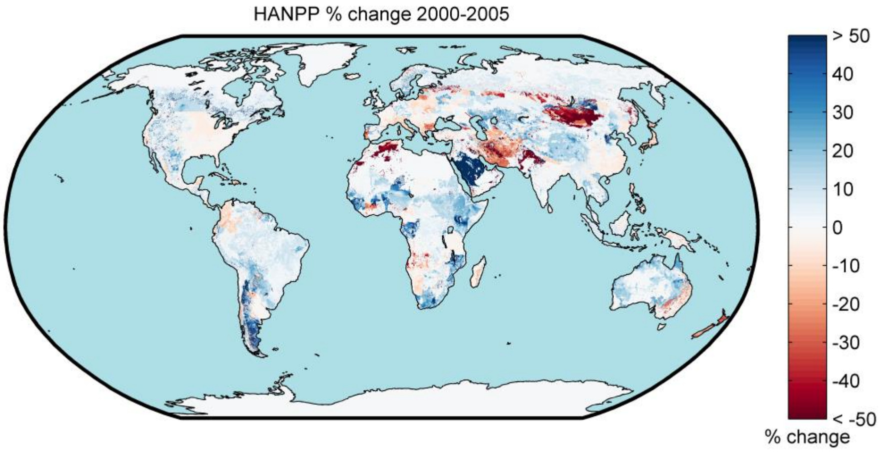

Figure 15: Changes of HANPP % NPP_{pot} between 2000 and 2005 as percentage of change. The red colour gradient indicates decreasing HANPP.

Figure 16 shows the **IPAT** relation, approximated by the relation between changes of HANPP and changes in several input-parameters, in order to scrutinize the influence of socio-economic changes on HANPP patterns. Here, HANPP changes between 2000 and 2005 (Figure 16) are used as a proxy for environmental impacts (**I**), which we correlate with population changes (**P**opulation), GDP changes (**A**ffluence), and changes of nitrogen inputs as well as change in areas equipped with irrigation infrastructure as proxies for technological change (**T**echnology). We rescaled all input variables that were available at 5min resolution to a 0.5° pixel size in order to match the resolution of the GDP and nitrogen-input datasets. We calculated the Pearson correlation coefficient (r) for all gridcells covered by a raster of 5° gridcell-bins. The correlation coefficient was “written” to the centre of the 5°-bin, after which the bin-window was moved to the next gridcell. This approach was inspired Carvalhais et al. (2014).

Results reveal strong correlations between changes of HANPP with population and GDP changes, particularly in Sub-Saharan Africa, where apparently population growth and rising GDP was followed by increased land-use impacts. Otherwise, nitrogen inputs revealed the most stringent correlation with

HANPP changes. Here, North America and Central America appear as hotspots of nitrogen increases, which coincided with decreasing HANPP- a sign of land use intensification that is characterized by increasing input-intensity on agricultural lands, while land use pressure is reduced, i.e. through forest regrowth and abandonment of marginal lands. In Sub-Saharan Africa and central Asia nitrogen inputs increased together with HANPP % NPP_{pot}, a typical pattern of land-use intensification in its initial stages (Krausmann et al. 2012; Gingrich et al. 2015).

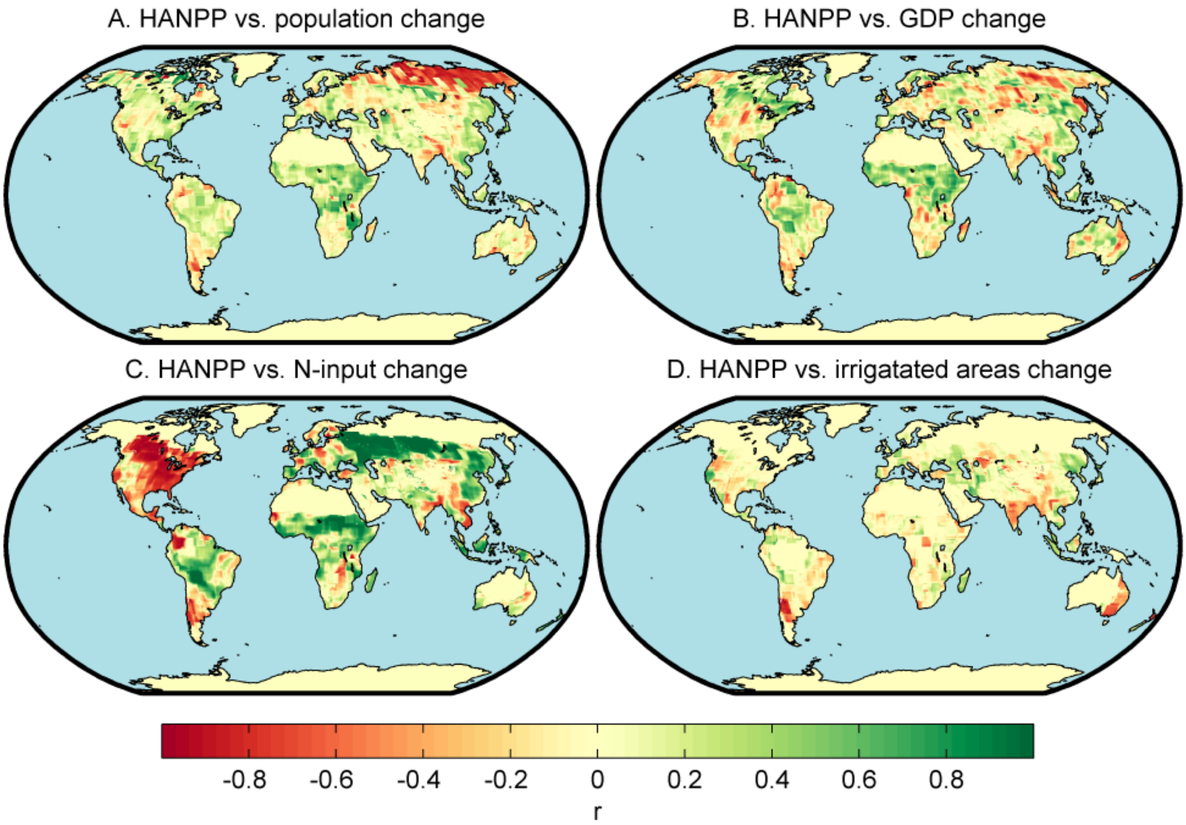

Figure 16: Correlation coefficient (r Pearson) of changes in HANPP % NPP_{pot} with changes of four different input variables between 2000 and 2005. A) population changes, B) GDP changes, C) changes of nitrogen inputs and D) changes of areas equipped with irrigation infrastructure. We calculated the Pearson correlation coefficient between 0.5° gridcells separately for bins of 5° gridcells. The correlation coefficient was "written" to the centre pixel of the 5°-bin, after which the bin-window was moved forward in 0.5° steps to the next gridcells.

4. Uncertainty of NPP_{pot}

Data uncertainty is naturally a problem for a global, centennial study that integrates so many different data sets, all of which have their own uncertainty issues. In general, we are confident that the robustness of our results has increased over time, due to better availability of "real-world" statistical data and remote sensing data in recent years, while the reliance on model-assumptions to fill data gaps increased back in time. For the details, please refer to the original data sets used here (Krausmann et al. 2013; Klein Goldewijk 2016; Sitch et al. 2003b).

A different type of uncertainty is, however, related to NPP_{pot} results, as these are model-derived and unlike the other parameters used here, are prone to uncertainties inherited in the model architecture. In order to assess the possible uncertainty range of our HANPP results attributed to NPP_{pot}, we calculated an alternative run of global HANPP, using NPP_{pot} outputs from LPJ-GUESS (Smith et al. 2001, 2014a), which is hitherto termed NPP_{pot_alt}.

Global HANPP % NPP_{pot_alt} trajectories (Figure 17 A) compare well and are almost identical to HANPP % NPP_{pot} (Figure 1 B), however, major difference between both runs prevail in the eleven world regions analysed here (Figure 17 A, B, C). Particularly Northern Africa and Western Asia, as well as Southern Asia reveal much higher levels of NPP_{pot} in the alternative run, which translated into lower HANPP levels as well (Figure 17 B, C). Similar trends are found in Sub-Saharan Africa and Oceania and Australia, though the differences between the HANPP % NPP_{pot} and HANPP % NPP_{pot_alt} were more moderate.

HANPP % NPP_{pot_alt} compared well the HANPP % NPP_{pot} in Southeast Asia, Central Asia and Russian Federation, and Western Europe, where the two NPP_{pot} models yielded similar results (Figure 17 B). In the remaining world regions, HANPP % of NPP_{pot} was lower in the alternative run (due to lower NPP_{pot}_alt; Figure 17 B).

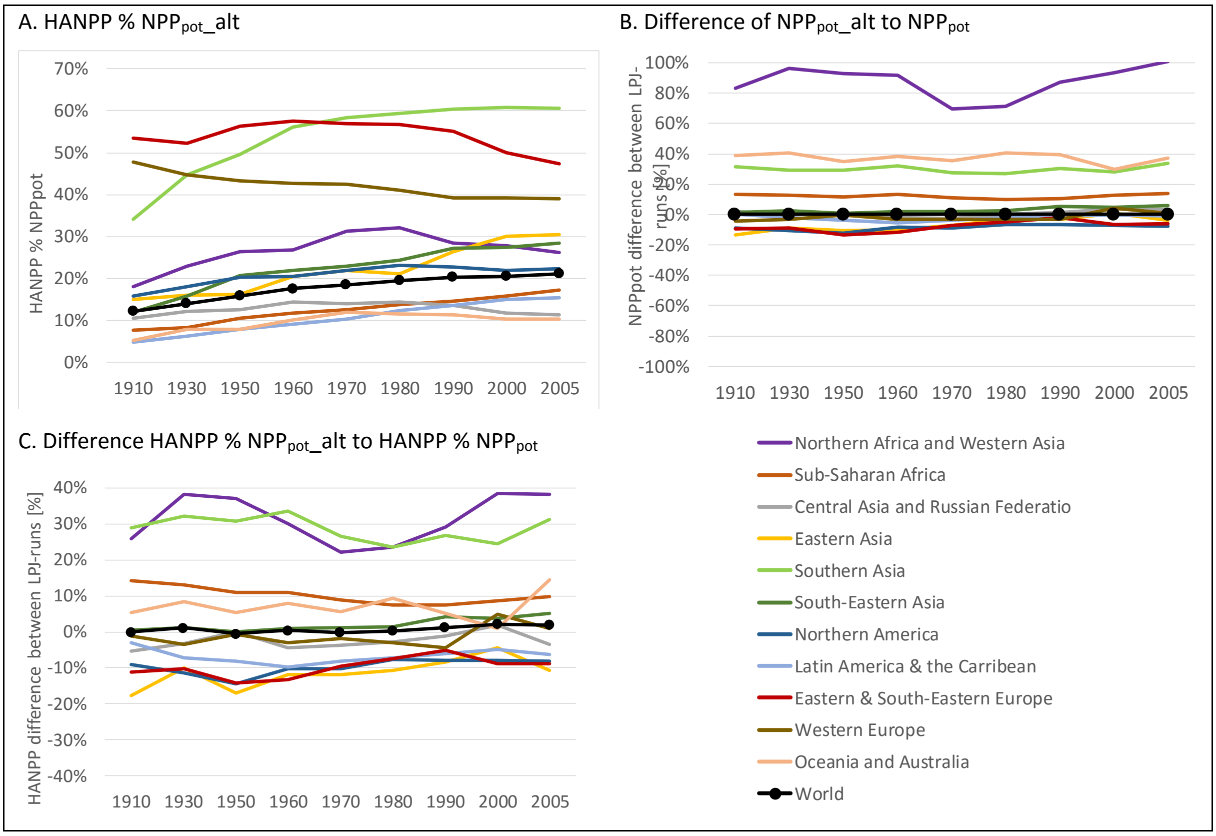

Figure 17: HANPP % of NPP_{pot} calculated with an alternative NPP_{pot}-model (LPJ-GUESS) broken down to eleven world regions. A. trends of HANPP % NPP_{pot}; B. Difference of HANPP % NPP_{pot} between results using LPJ-GDVM (this study) and the alternative NPP_{pot}_alt (LPJ-GUESS run).

The differences in terms of spatial patterns between the two HANPP versions reveal water-limited areas to be most affected by NPP_{pot} uncertainties, as it is demonstrated by NPP_{pot_alt}, which was more than twice as high in Australia, the Sahel-belt, Western US and parts of central Asia. In contrast, NPP_{pot_alt} was much lower in the temperature (and precipitation)-limited areas of the Northern hemisphere, as is visible in Canada and parts of Siberia.

As these areas are, by definition, prone to very low NPP_{pot}, the striking differences between the two NPP_{pot} versions do not translate into relevant differences of absolute NPP_{pot} levels globally (Figure 17 B). However, as the BACI-index focuses on changes in essential biosphere-atmosphere variables, such "small-number problems" are in fact important. Hence, in the BACI-context uncertainties of model-derived parameters for such regions should be given special attention. Furthermore, as dry-land areas are dominated by grazing lands (refer to the appendix, Figure A4 B), the uncertainties related to NPP flows uncovered here, directly add to the uncertainties of grazing land use and particularly to the allocation of grazed NPP in the world's dryland regions (Fetzel et al. 2017; Erb et al. 2016).

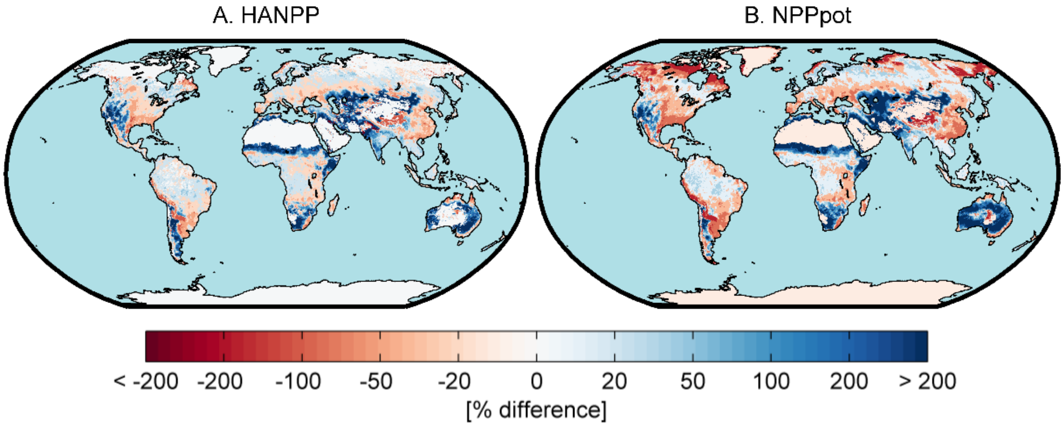

Figure 18: Spatial differences of HANPP and NPP_{pot} between results calculated with LPJ-GDVM and LPJ-GUESS. A. Differences in HANPP % NPP_{pot}, B. differences in NPP_{pot}. The differences are expressed in %, where positive values (blue color gradient) indicate that NPP_{pot} was lower than NPP_{pot_alt} and negative values (red color gradient) indicate the opposite.

5. Link to BACI downstream indicators

This report represents an in-depth, spatially explicit analysis of global land-use and related biomass-flows at a five minutes (ca. 10x10 km^2 at the equator) resolution between 1910 and 2005. We have found significant shifts of land use patterns over the past 100 years, both in terms of the intensity and spatial allocation of land use. Our results and data sets are directly usable in the BACI-context, particularly in WP6 and WP7 which focus on the validation of hotspots detected by BACI and its downstream products based on independent socio-economic and climatic (refer to WP6) data sets.

The data sets compiled here represent a central data source for integrating the socio-economic dimension of biosphere atmosphere changes into BACI and particularly for scrutinizing drivers of biosphere-atmosphere changes related to land use. Using the HANPP framework as an analytical tool is extremely beneficial in this regard, because by implementing NPP_{pot} as a reference system for current land use impacts, HANPP allows highlighting the socio-economic dimension of land use, while climatic and bio-geographic factors are neutralized, because they are subsumed in the NPP_{pot} signal. For instance, considering changes of actual NPP only, it is intricate, if not impossible, to distinguish climatic from socio-economic drivers of NPP changes. A decrease of cropland NPP, for instance, could be an effect either of drought, or of decreasing cropland use intensity. However, when cropland NPP is related to its natural counterpart NPP_{pot} (which would decrease in the case of a drought), decreasing NPP_{act} % NPP_{pot} would clearly indicates a shift in land use. Contrary, constant NPP_{act} % NPP_{pot}, would hint to effects of climatic changes on cropland NPP. This is, for instance, visible in the comparison of Figure 8D and Figure 9D, where the HANPP levels per area (in $gC/m^2/yr$) reveal a more dynamic pattern of hot-and coldpots (Figure 8D) than HANPP expressed as % of NPP_{pot} (Figure 9D).

NPP flows, which are used as a quantitative unit in the HANPP framework, are directly related to a set of essential ecosystem variables as planned outputs of the BACI project, in particular to GPP, biomass, FaPAR, or water use efficiency. Hence, the ability of the HANPP assessment to distinguish natural from “human” induced drivers of NPP changes, will indirectly facilitate a better interpretation of changes in the mentioned BACI downstream products. The centennial data presented here even allow for analysing the relevance of climatic versus socio-economic drivers of NPP changes in a long-term perspective. Hence, shifts within the BACI period (2000 onwards) can be checked for their relevance by putting them in the long-term perspective of shifts within more than 100 years.

Furthermore our findings on HANPP and its components $HANPP_{harv}$ and $HANPP_{luc}$ reveal that land conversion (approximated by $HANPP_{luc}$ changes) dominated recent land use trends (2000-2005 period) in some world region (predominantly the developing countries of Sub-Saharan Africa), while harvest and particularly land-use intensification play a dominant role in the industrialized world and in the biomass-exporting countries. This is relevant for the BACI-context, as such changes in land-use intensification are not easily, if at all, detectable by remote sensing techniques. Hence, the data set presented here allows unravelling components of biosphere-atmosphere change that are beyond changes of spectral signals, but that occur at the heart of societal change, such as economic and technological change and population dynamics. This is also supported by the strong correlations of HANPP increases with technological inputs and population growth between 2000 and 2005, particularly in Sub-Saharan Africa (Figure 16).

Our results on NPP_{pot} uncertainties revealed the world's water limited areas as hotspots of uncertainties. Particularly model-derived metrics must treat such areas with care, as it is apparently intricate to capture the high dynamics of these areas related to changes in water availability on an annual and sub-annual basis. Particular attention must hence be given to these areas when it comes to scrutinizing hot-and coldspots of biosphere-atmosphere change and when relating them to socio-economic and natural drivers.

6. References

Bartels, L. E., 2013: Socio-ecological impacts of land grabbing for nature conservation on a pastoral community: A HANPP-based case study in Ololosokwan Village, Northern Tanzania. Social Ecology Working Paper, https://www.aau.at/wp-content/uploads/2016/11/working-paper-149-web.pdf.

Boserup, E., 1965: The conditions of agricultural growth. The economics of agrarian change under population pressure. Aldine/Earthscan, Chicago,.

Carvalhais, N., and Coauthors, 2014: Global covariation of carbon turnover times with climate in terrestrial ecosystems. Nature,. http://www.nature.com/nature/journal/vaop/ncurrent/full/nature13731.html (Accessed March 6, 2015).

Commoner, B., 1972: The environmental cost of economic growth. Chem. Br., **8**, 52.

Ehrlich, P. R., and J. P. Holdren, 1971: Impact of population growth. http://www.agro.uba.ar/users/fernande/EhrlichHoldren1971impactPopulation.pdf (Accessed November 18, 2015).

Ellis, E. C., and N. Ramankutty, 2008: Putting people in the map: anthropogenic biomes of the world. Front. Ecol. Environ., **6**, 439–447.

——, J. O. Kaplan, D. Q. Fuller, S. Vavrus, K. K. Goldewijk, and P. H. Verburg, 2013: Used planet: A global history. Proc. Natl. Acad. Sci., **110**, 7978–7985.

Erb, K. H., F. Krausmann, V. Gaube, S. Gingrich, A. Bondeau, M. Fischer-Kowalski, and H. Haberl, 2009: Analyzing the global human appropriation of net primary production–processes, trajectories, implications. An introduction. Ecol. Econ., **69**, 250–259.

Erb, K.-H., V. Gaube, F. Krausmann, C. Plutzar, A. Bondeau, and H. Haberl, 2007: A comprehensive global 5 min resolution land-use data set for the year 2000 consistent with national census data. J. Land Use Sci., **2**, 191–224.

——, H. Haberl, M. R. Jepsen, T. Kuemmerle, M. Lindner, D. Müller, P. H. Verburg, and A. Reenberg, 2013: A conceptual framework for analysing and measuring land-use intensity. Curr. Opin. Environ. Sustain.,. http://www.sciencedirect.com/science/article/pii/S1877343513000894.

——, T. Fetzel, T. Kastner, C. Kroisleitner, C. Lauk, A. Mayer, and M. Niedertscheider, 2016: Livestock grazing, the neglected land use. Social Ecology, Springer, 295–313 http://link.springer.com/chapter/10.1007/978-3-319-33326-7_13.

FAO, 2017: FAOSTAT: Statistical Database of the United Nations Food and Agricultural Organization. http://faostat.fao.org/,.

Fetzel, T., M. Niedertscheider, H. Haberl, F. Krausmann, and K.-H. Erb, 2016: Patterns and changes of land use and land-use efficiency in Africa 1980-2005: an analysis based on the human appropriation of net primary production framework. Reg. Environ. Change, **16**, 1507.

——, P. Havlik, M. Herrero, and K.-H. Erb, 2017: Seasonality constraints to livestock grazing intensity. Glob. Change Biol., **23**, 1636–1647.

Foley, J. A., and Coauthors, 2005: Global consequences of land use. science, **309**, 570–574.

Garnett, T., and Coauthors, 2013: Sustainable intensification in agriculture: premises and policies. Science, **341**, 33–34.

Gingrich, S., and Coauthors, 2015: Exploring long-term trends in land use change and aboveground human appropriation of net primary production in nine European countries. Land Use Policy, **47**, 426–438, doi:10.1016/j.landusepol.2015.04.027.

Haberl, H., and Coauthors, 2007: Quantifying and mapping the human appropriation of net primary production in earth's terrestrial ecosystems. Proc. Natl. Acad. Sci., **104**, 12942.

Haberl, H., K.-H. Erb, and F. Krausmann, 2014: Human appropriation of net primary production: patterns, trends, and planetary boundaries. Annu. Rev. Environ. Resour., **39**, 363–391.

Hostert, P., T. Kuemmerle, A. Prishchepov, A. Sieber, E. F. Lambin, and V. C. Radeloff, 2011: Rapid land use change after socio-economic disturbances: the collapse of the Soviet Union versus Chernobyl. Environ. Res. Lett., **6**, 045201.

IAASTD, 2009: Agriculture at a Crossroads. International Assessment of Agricultural Knowledge, Science and Technology for Development (IAASTD), Global Report. Island Press, Washington, D.C.,.

Jepsen, M. R., and Coauthors, 2015: Transitions in European land-management regimes between 1800 and 2010. Land Use Policy, **49**, 53–64.

Kastner, T., 2009: Trajectories in human domination of ecosystems: Human appropriation of net primary production in the Philippines during the 20th century. Ecol. Econ., **69**, 260–269.

——, K.-H. Erb, and S. Nonhebel, 2011: International wood trade and forest change: A global analysis. Glob. Environ. Change, **21**, 947–956.

——, ——, and H. Haberl, 2015: Global human appropriation of net primary production for biomass consumption in the European Union, 1986–2007. J. Ind. Ecol., **19**, 825–836.

Klein Goldewijk, C. G. M., 2016: A historical land use data set for the Holocene; HYDE 3.2 (replaced). doi:10.17026/dans-znk-cfy3.

Krausmann, F., and Coauthors, 2012: Long-term trajectories of the human appropriation of net primary production: Lessons from six national case studies. Ecol. Econ., **77**, 129–138, doi:10.1016/j.ecolecon.2012.02.019.

——, and Coauthors, 2013: Global human appropriation of net primary production doubled in the 20th century. Proc. Natl. Acad. Sci.,. http://www.pnas.org/content/early/2013/05/30/1211349110.short (Accessed June 21, 2013).

Kuemmerle, T., and Coauthors, 2011: Post-Soviet farmland abandonment, forest recovery, and carbon sequestration in western Ukraine. Glob. Change Biol., **17**, 1335–1349.

——, and Coauthors, 2013: Challenges and opportunities in mapping land use intensity globally. Curr. Opin. Environ. Sustain., **5**, 484–493.

Lambin, E. F., and P. Meyfroidt, 2011: Global land use change, economic globalization, and the looming land scarcity. Proc. Natl. Acad. Sci., **108**, 3465–3472.

Lindenmayer, D., S. Cunningham, and A. Young, 2012: Land use intensification: Effects on agriculture, biodiversity and ecological processes. CSIRO publishing.

Lu, C., and H. Tian, 2017: Global nitrogen and phosphorus fertilizer use for agriculture production in the past half century: shifted hot spots and nutrient imbalance. Earth Syst. Sci. Data, **9**, 181–192, doi:https://doi.org/10.5194/essd-9-181-2017.

Luyssaert, S., and Coauthors, 2014: Land management and land-cover change have impacts of similar magnitude on surface temperature. Nat. Clim. Change, **4**, 389–393.

Mather, A. S., 2001: The transition from deforestation to reforestation in Europe. Agric. Technol. Trop. Deforestation, 35–52.

Matson, P. A., and P. M. Vitousek, 2006: Agricultural intensification: will land spared from farming be land spared for nature? Conserv. Biol., **20**, 709–710.

Meyfroidt, P., and E. F. Lambin, 2011: Global forest transition: prospects for an end to deforestation. http://www.annualreviews.org/eprint/DMDIR7h9j2hkf9VTaIsG/full/10.1146/annurev-environ-090710-143732.

Millenium Ecosystem Assessment, 2005: Ecosystems and Human Well-Being - Our Human Plante. Summary for Decision Makers. Island Press, Washington, D.C.,.

Musel, A., 2009: Human appropriation of net primary production in the United Kingdom, 1800 - 2000. Changes in society's impact on ecological energy flows during the agrarian-industrial transition. Ecol. Econ., **69**, 270–281.

Niedertscheider, M., and K. Erb, 2014: Land system change in Italy from 1884 to 2007: Analysing the North–South divergence on the basis of an integrated indicator framework. Land Use Policy, **39**, 366–375.

——, S. Gingrich, and K.-H. Erb, 2012: Changes in land use in South Africa between 1961 and 2006: an integrated socio-ecological analysis based on the human appropriation of net primary production framework. Reg. Environ. Change, **12**, 715–727, doi:10.1007/s10113-012-0285-6.

——, T. Kuemmerle, D. Müller, and K.-H. Erb, 2014: Exploring the effects of drastic institutional and socio-economic changes on land system dynamics in Germany between 1883 and 2007. Glob. Environ. Change, **28**, 98–108.

——, and Coauthors, 2016a: Africa's Land System Trajectories 1980–2005. Social Ecology, Springer, 361–373 http://link.springer.com/chapter/10.1007/978-3-319-33326-7_17.

——, T. Kastner, T. Fetzel, H. Haberl, C. Kroisleitner, C. Plutzar, and K.-H. Erb, 2016b: Mapping and analysing cropland use intensity from a NPP perspective. Environ. Res. Lett., **11**, 014008.

Nordhaus, W. D., 2005: Geography and Macroeconomics: New Data and New Findings. Proc. Natl. Acad. Sci. U. S. Am. PNAS, **103**. http://dx.doi.org/10.1073/pnas.0509842103.

——, and X. Chen, 2016: Global Gridded Geographically Based Economic Data (G-Econ), Version 4. NASA Socioeconomic Data and Applications Center (SEDAC), Palisades, NY, http://doi.org/10.7927/H42V2D1C.

Olson, D. M., and Coauthors, 2001: Terrestrial Ecoregions of the World: A New Map of Life on Earth A new global map of terrestrial ecoregions provides an innovative tool for conserving biodiversity. BioScience, **51**, 933–938.

Plutzar, C., and Coauthors, 2015: Changes in the spatial patterns of human appropriation of net primary production (HANPP) in Europe 1990–2006. Reg. Environ. Change, 1–14, doi:10.1007/s10113-015-0820-3.

Prishchepov, A. V., V. C. Radeloff, M. Baumann, T. Kuemmerle, and D. Müller, 2012: Effects of institutional changes on land use: agricultural land abandonment during the transition from state-command to market-driven economies in post-Soviet Eastern Europe. Environ. Res. Lett., **7**, 024021.

Ramankutty, N., and J. A. Foley, 1999: Estimating historical changes in global land cover: Croplands from 1700 to 1992. Glob. Biogeochem. Cycles, **13**, 997–1027.

Rudel, T. K., O. T. Coomes, E. Moran, F. Achard, A. Angelsen, J. Xu, and E. Lambin, 2005: Forest transitions: towards a global understanding of land use change. Glob. Environ. Change, **15**, 23–31.

Sanderson, E. W., M. Jaiteh, M. A. Levy, K. H. Redford, A. V. WANNEBO, and G. Woolmer, 2009: The Human Footprint and the Last of the Wild. BioScience, **52**, 891–904.

Siebert, S., M. Kummu, M. Porkka, P. Döll, N. Ramankutty, and B. R. Scanlon, 2015: A global data set of the extent of irrigated land from 1900 to 2005. Hydrol. Earth Syst. Sci., **19**, 1521–1545.

Simons, H., and Coauthors, 2001: Global ecological zoning for the Global Forest Resources Assessment 2000-Final report. http://www.citeulike.org/group/15400/article/12205414.

Sitch, S., and Coauthors, 2003a: Evaluation of ecosystem dynamics, plant geography and terrestrial carbon cycling in the LPJ dynamic global vegetation model. Glob. Change Biol., **9**, 161–185, doi:10.1046/j.1365-2486.2003.00569.x.

Sitch, S., and Coauthors, 2003b: Evaluation of ecosystem dynamics, plant geography and terrestrial carbon cycling in the LPJ dynamic global vegetation model. Glob. Change Biol., **9**, 161–185.

Smith, B., I. C. Prentice, and M. T. Sykes, 2001: Representation of vegetation dynamics in the modelling of terrestrial ecosystems: comparing two contrasting approaches within European climate space. Glob. Ecol. Biogeogr., **10**, 621–637.

Smith, B., D. Wårlind, A. Arneth, T. Hickler, P. Leadley, J. Siltberg, and S. Zaehle, 2014a: Implications of incorporating N cycling and N limitations on primary production in an individual-based dynamic vegetation model. Biogeosciences, **11**, 2027–2054, doi:10.5194/bg-11-2027-2014.

Smith, P., and Coauthors, 2014b: Agriculture, forestry and other land use (AFOLU). http://pure.iiasa.ac.at/11115/.

Smith, W. K., C. C. Cleveland, S. C. Reed, and S. W. Running, 2014c: Agricultural conversion without external water and nutrient inputs reduces terrestrial vegetation productivity. Geophys. Res. Lett., **41**, 449–455.

Steffen, W., and Coauthors, 2015: Planetary boundaries: Guiding human development on a changing planet. Science, 1259855, doi:10.1126/science.1259855.

Tilman, D., C. Balzer, J. Hill, and B. L. Befort, 2011: Global food demand and the sustainable intensification of agriculture. Proc. Natl. Acad. Sci., **108**, 20260–20264.

Verburg, P. H., O. Mertz, K.-H. Erb, H. Haberl, and W. Wu, 2013: Land system change and food security: towards multi-scale land system solutions. Curr. Opin. Environ. Sustain., **5**, 494–502.

Vitousek, P. M., H. A. Mooney, J. Lubchenco, and J. M. Melillo, 1997: Human domination of Earth's ecosystems. Science, **277**, 494.

Zika, M., and K.-H. Erb, 2009: The global loss of net primary production resulting from human-induced soil degradation in drylands. Ecol. Econ., **69**, 310–318, doi:10.1016/j.ecolecon.2009.06.014.

Appendix

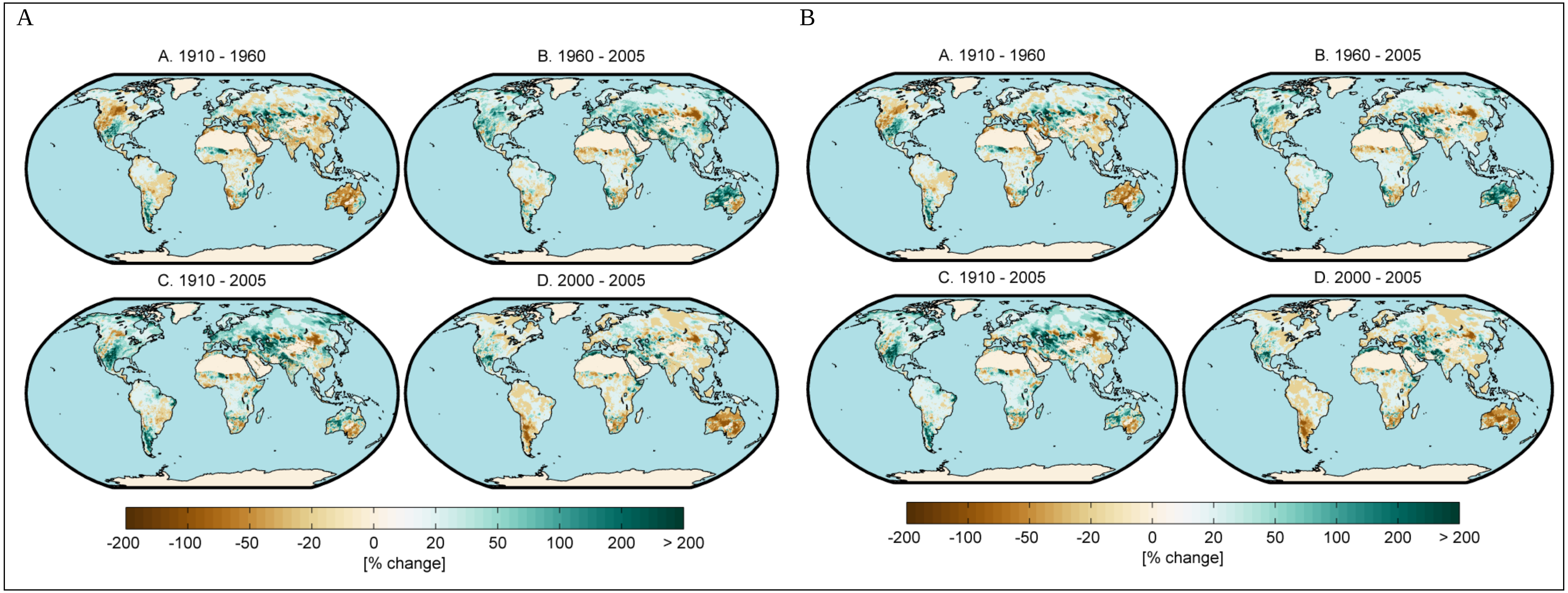

Figure A1. Changes of NPP_{act} [gC/m2/yr] (A) and NPP_{pot} (B) in percent absolute change from A 1910-1960, B 1960-2005, C. 1910-2005 and D. 2000-2005.

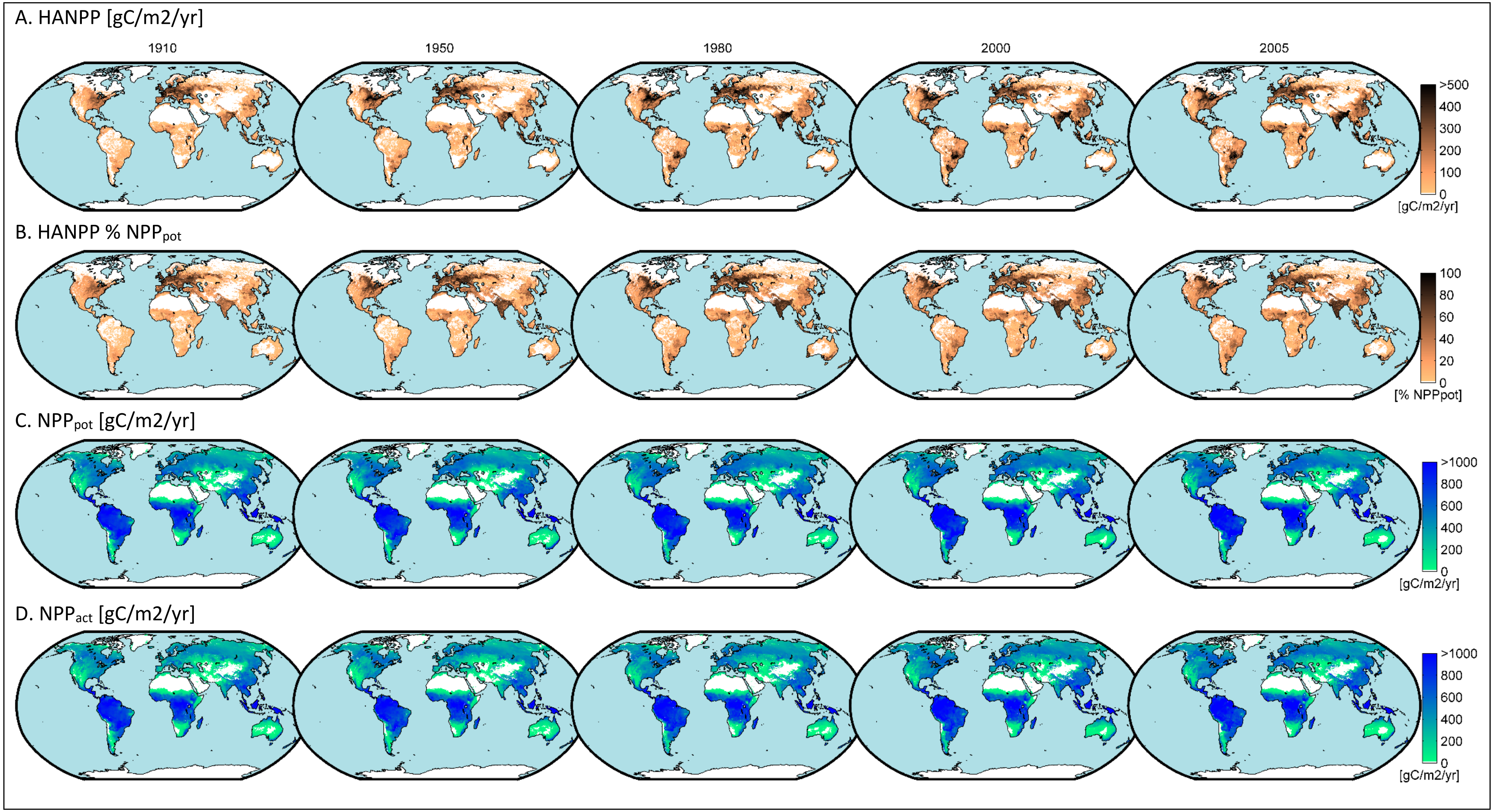

Figure A2: Time cuts for the years 1910, 1950, 1980, 2000 and 2005 of A. HANPP per area, B. HANPP % NPP_{pot}, C. NPP_{pot} per area and D. NPP_{act} per area

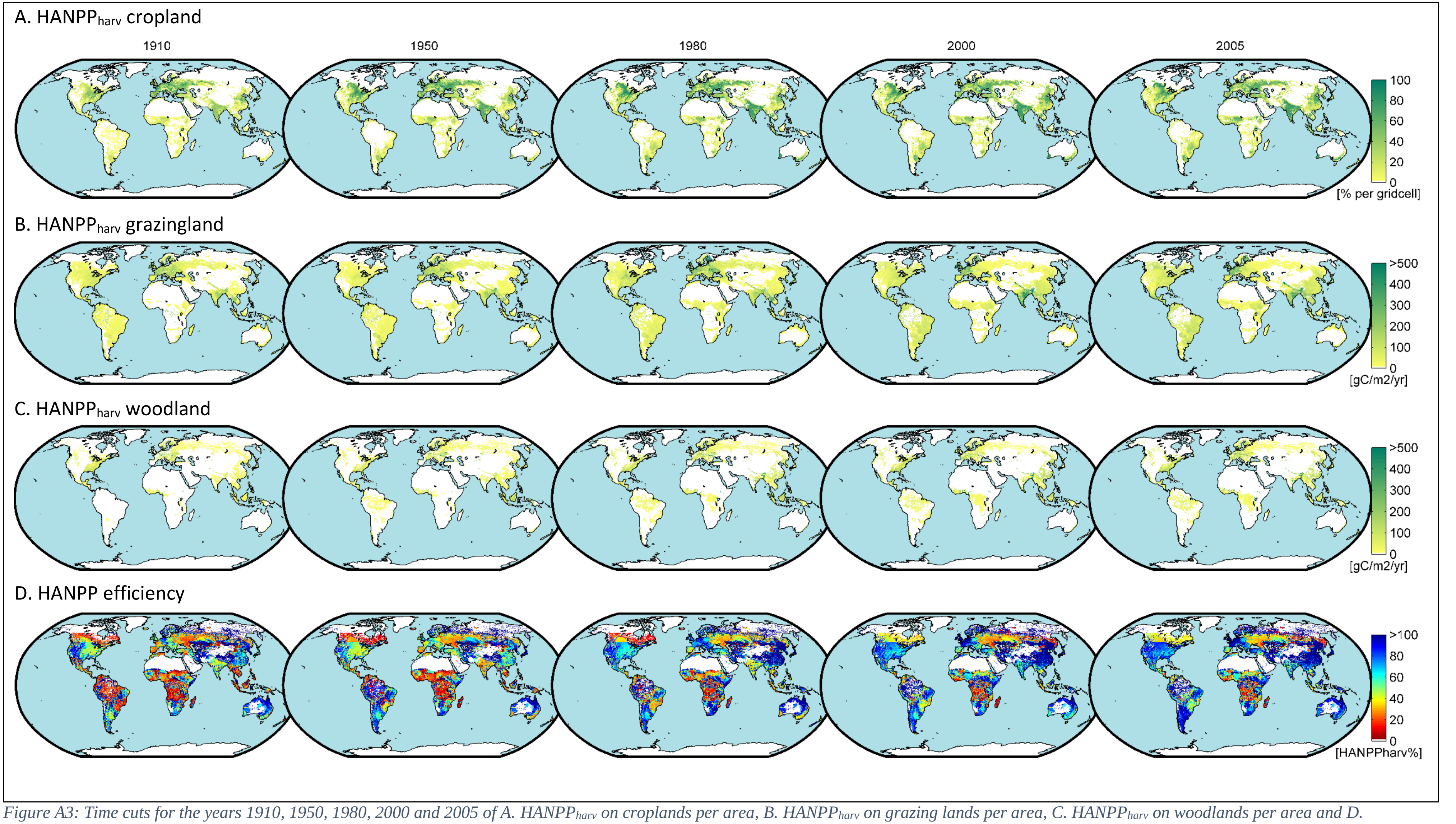

Figure A3: Time cuts for the years 1910, 1950, 1980, 2000 and 2005 of A. HANPP$_{harv}$ on croplands per area, B. HANPP$_{harv}$ on grazing lands per area, C. HANPP$_{harv}$ on woodlands per area and D. HANPP efficiency, calculated as the share of HANPP$_{harv}$ to total HANPP.

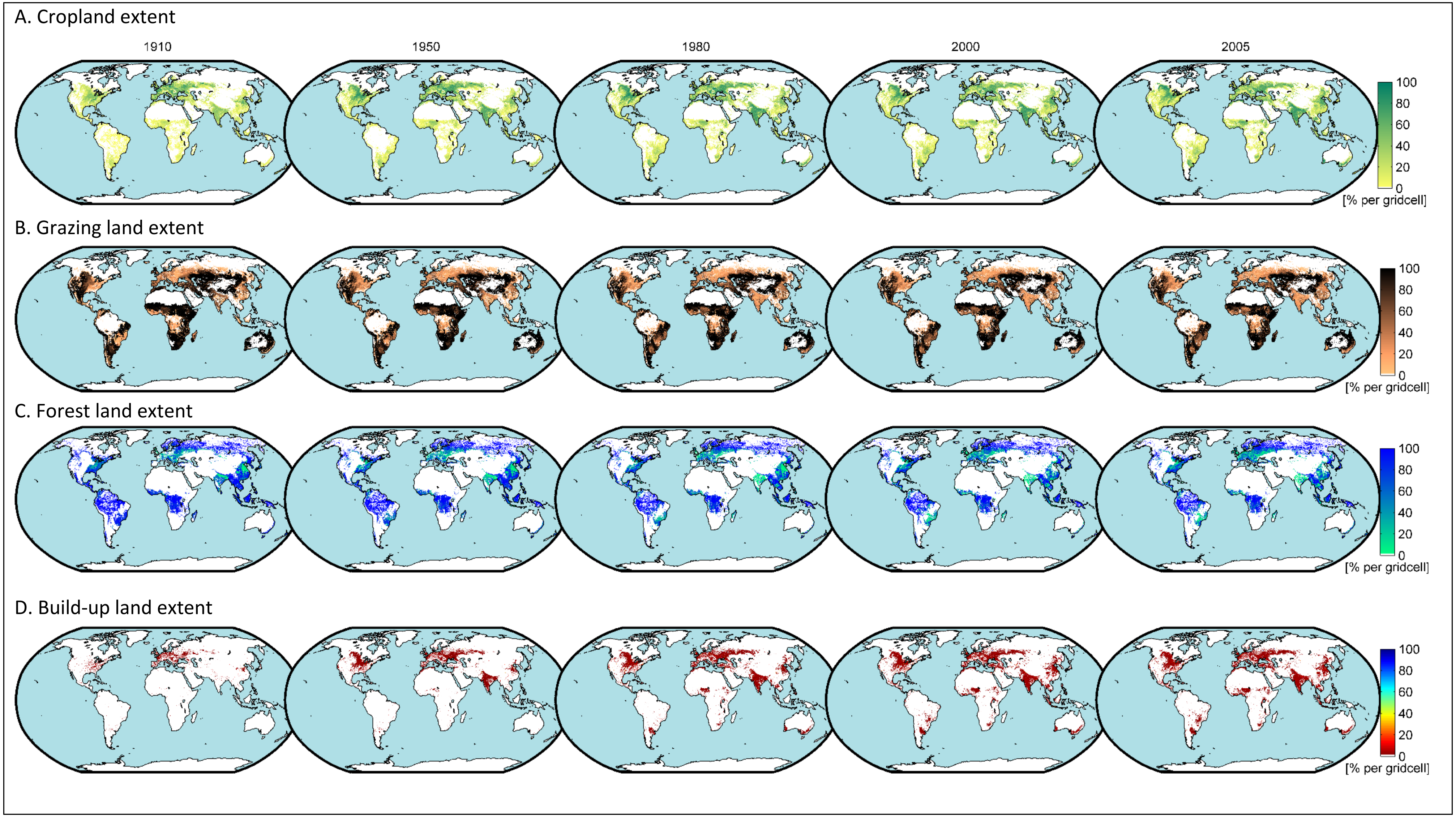

Figure A4: Time cuts for the years 1910, 1950, 1980, 2000 and 2005 of A. cropland extent, B. grazing land extent, C. woodland extent and D. build-up area extent.